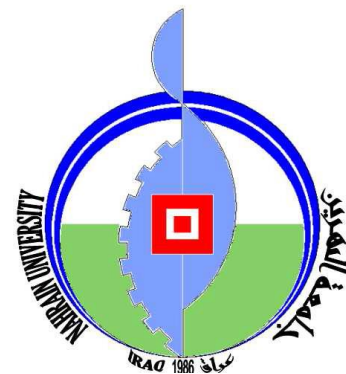**Republic of Iraq**
Ministry of Higher Education
and Scientific Research
AL-Nahrain University
College of Science
Department of physics

Design and Fabrication of Antireflection ZnO Thin Film by Using Different Techniques

A Thesis

Submitted to the College of Science, Al-Nahrain University in Partial Fulfillment of the Requirements for Degree of Master of Science in Physics.

By

Nidaa Taha Yaseen

B.Sc., Mustansiriya University (2005)

Supervised by

Dr. Alaa J. Ghazai

(Assistant prof)

July 2017   shawal 1438

بسم الله الرحمن الرحيم

إِنَّا فَتَحْنَا لَكَ فَتْحًا مُبِينًا

صدق الله العلي العظيم

سورة الفتح الآية 1

Supervisors Certification

We certify that this thesis was prepared by *Nidaa Taha Yaseen* under our supervision at the Physics Department, College of Science, University of AI Nahrain as partial requirement for the degree of Master of science in physics.

Signature:

Name: **Dr. Alaa Jabbar Ghazai**

Scientific Degree: **Assistant Professor**

Date: 25 / 7 /2017

In view of the available recommendation, I forward this for debate by the examination committee.

Signature:

Name: **Dr.Saad Naji Abood**

Title: Professor

Title: Head of Physics Science Department

College of Science / Al Nahrain University.

Date: 26 / 7 /2017

Committee Certification

We, the examining committee certify that we have read this thesis entitled "Design and fabrication of antireflection coating thin film by using different technique" and examined the student "Nidaa Taha Yaseen" in its contents and that in our opinion; it is accepted for the Degree of Master of Science in physics.

Signature:

Name: **Dr. Aliyah Abdul Mhsin Shehab**

Scientific Degree: Professor

Date:^{24}/7/ 2017

(Chairman)

Signature:

Name: Dr. **Osama A. Dakhil**

Scientific Degree: Assist Prof.

Date:^{24}/7/ 2017

(Member)

Signature:

Name: Dr. **Qased A. Salih**

Scientific Degree: Assist Prof.

Date:23/7/ 2017

(Member)

Signature:

Name: **Dr. Alaa Jabbar Ghazai**

Scientific Degree: Assist Professor

Date23/7/ 2017

(Member/ **Supervised**)

I, hereby certify upon the decision of the examining committee.

Signature:

Name: **Dr. Hadi M. A. Abood**

Scientific Degree: **Professor**

Title: Dean of College of Science

Date:20/7/ 2017

DEDICATION

TO

MY, FATHER AND MOTHER SOIL (ALLAH MERCY), DAUGHTER SHAMS, BROTHERS, AND FAMILY

ACKNOWLEDGEMENTS

List of Contents

Contents	

4.4.Scanning Electron Microscopes (SEM) Results		48
4.5.Optical Properties		59
4.6 Optical Properties Results of ZO Nanoparticle by Sol-Gel Technique		66
Chapter Five Conclusion and Future Works		
5.1.Conclusion		68
5.2.Future Works		68
References		

List of Symbols

Symbols	Description	Units
A	Absorption	-
ARCs	Antireflection coating system	-
$\overline{E}$	Electric field vector	N/Colum
$\overline{H}$	Magnetic field vector	Tesla
J	Current density	Amp/m^2
K	Wave vector	1/nm
N	Imaginary part of refractive index	-
n	Real part of refractive index	-
σ	Conductivity	Siemens/m
R	Reflection	Siemens/m
r*	Reflection coefficient	-
$\overline{S}$	Panting vector	-
T	Transmission	-
ω	Angler momentum	nt.m.s
ε	Dielectric constant (Permeability)	Fm^{-1}
μ	Permittivity	Mm^{-1}
α	Absorption coefficient	cm^{-1}
λ	Wavelength	nm or A^0
$λ_d$	Design wavelength	nm or A^0
FE	Field emission	
Eg	Energy gap	eV

List of Abbreviations

Symbol	Description
FWHM	Full width at half maximum
XRD	X-ray diffraction
RT	Room temperature
SEM	Scanning Electron Microscopy
UV-VIS	Ultraviolet- Visible
EDX	Energy dispersive X-ray
ECE	Electrochemical etching method
RCA	Regular Cleaning American
MEA	Monoethanol amine
DW	Distilled water
ASTM	American Standard of Testing Materials
V.B	Valance band
C.B	Condition band
QD_S	Quantum dots
PLA	Pulse laser ablation
SRO	Short range order
DOS	Density of state

Summary

In this work single layer antireflection coating of ZnO thin film has been designed and fabrication on glass and PSi substrates using pulse laser ablation (PLA) and spin coating techniques.

Mainly, the work, divided into two parts, first: single antireflection of ZnO thin film using modified characteristics matrix to satisfy zero reflection condition theoretically. Second: ZnO nanoparticle deposited on different substrates using PLA which including the effect of duration pulse of 1000, 1500, 2000 pulses, Energy of 600, 700, 800 mJ and type of solvent by methanol and distilled water have been fabricated studied. In addition, spin coating method have been employed to synthesis this film.

Structural and optical properties of prepared films have been characterized using XRD, SEM and EDX, and UV-Vis, respectively. XRD results revealed that the ZnO thin film have hexagonal structure with polycrystalline in nature with preferred orientation of (002). In addition, crystalline size was increased with the increasing of duration pulses at methanol solvent at fixed energy of 700 mJ, besides; in distilled water solvent at 700 mJ have low crystalline size at duration pulse of 1500 pulse. While at fixed duration of 1500 pulse, the crystalline size has low valne at energy of 700 mJ . As well as, the film deposited on glass and PSi substrate using sol gel method have crystalline size of (96.83and 85.16) nm respectively.

Narrow FWHM and no phase change has been observed in all cases. SEM images showed that for all cases the films were homogenous with some island and cluster then cracking started to obtain with the increasing of increase the pulse number. Expected of film on glass prepared using

PLA with methanol solvent of energy 700 mJ and pulse duration of 1500 pulse which showed nanostructure like tree leaf.

EDX analysis showed that the prepared films were free of defects and continmations.

Optical properties including optical behavior, optical band gap energy and absorption coefficient as a function of a wavelength revealed that the prepared film have high transmittance behavior around 85% at visible region ranged of 300-800 nm with high optical band gap energy of 3.37 eV with blue shift toward short wavelength.

Chapter One

Introduction

1.1 Introduction

In order to make size and structure dependent properties and phenomena, as distinct from those associated with individual atoms or molecules with bulk materials to manipulate and control matter in nanoscale, the nanotechnology have been applied. The term "nanoscale" is called on the structure size ranged from 1 to 100 nanometers (nm), which have great scientific interest as they are effectively a bridge between bulk materials and atomic or molecular structures. In this size, physical, chemical, and biological properties of substances are different from that of the micrometer and larger scales and these new properties of the materials, devices and systems could be develop unlimited [1,2]. There are two reasons for these unique properties could listed as following:

1- At the scale of nanometers, particles and structures have a very high surface-to-mass ratio. Makes them highly reactive compared to their bulk structure.

2- Nanometers exist in the term of quantum physics, and quantum properties are similarly valuable in developing enhanced materials [3].

In last a few years, zinc oxide (ZnO) nanostructure thin film have been attracted more attention due to the unusual properties of high transparency in the visible spectrum In addition , high chemical stability, excellent electrical and optical properties; with a wide band gap energy of 3.37 eV, which make it more suitable for short-wavelength optoelectronic applications [4,5]. Besides, ZnO has a large exciting binding energy of 60 mv at room temperature.

1.2 Antireflection Coating (ARC)

An anti-reflection coating (ARC) is widely used in most of the optical applications to reduce the unwanted reflection on the

surfaces   of   the   optical   components   [6]   which   improves   the efficiency   by reduce the light lost, it's consiste   of   a thin   layer   or multilayer, which may be isolating dielectric materials[7], metals, or a mixture of isolating materials.[8,9].   The main property of isolating films it's have low absorption ($\alpha < 10^3$ cm^{-1}) [7]

Anti-reflective   coatings   are   used   in   a   wide   variety   of applications such as anti-glare coatings on corrective lenses, camera lens elements, solar cells[7], arial   survy   camera, star sensors, and thermal imaging system[10].

The   anti-reflection   phenomenon has been define firstly by Rayleigh as results from the surfaces of optical components that are coated with a particular substance (using chemical methods)[11].

Early   references   to   the   science   of   thin   film   deposition include   the   research conducted   by   Michael   Faraday   in   1857. Faraday created thin metallic films which thermally induced evaporation using electrical heat resistance by allowed   an electric current to pass through a metallic wire and heat it to would evaporate[12].

1.3 Thin-Film Interference

Mathematical analysis of light interference at and through thin-film boundaries carry out using the relations that described the spread of the optical wave inside each layer on the interface that separate the layers . let's consider a light beam coming from a light source (S) fall on a thin film with a geometric   thickness of d at a point   (A). Nnaturally, part of the light will be reflected back to   the   same incident medium in the direction of the (1) ray and some will be transmitted towards (AF), and when it arrives to point F, part of this ray will reflect also to point B and   another part will be transmit towards H. as well as, at point B, the ray (FB) will continue

to split to a reflected part and a transmitted part, and so on In the result will get two groups of parallel rays on both sides of the film, the intensity on both groups will highly decreases from one ray to another, meaning that the first incident light has greater intensity than the following one and so on [13]. Both the reflected light and transmitted light inside the film have a direction and a value that depends on the nature and properties of the mediums, angle of incidence and the geometric thickness of the membrane (d). This process could be shown in Figure (1.1)
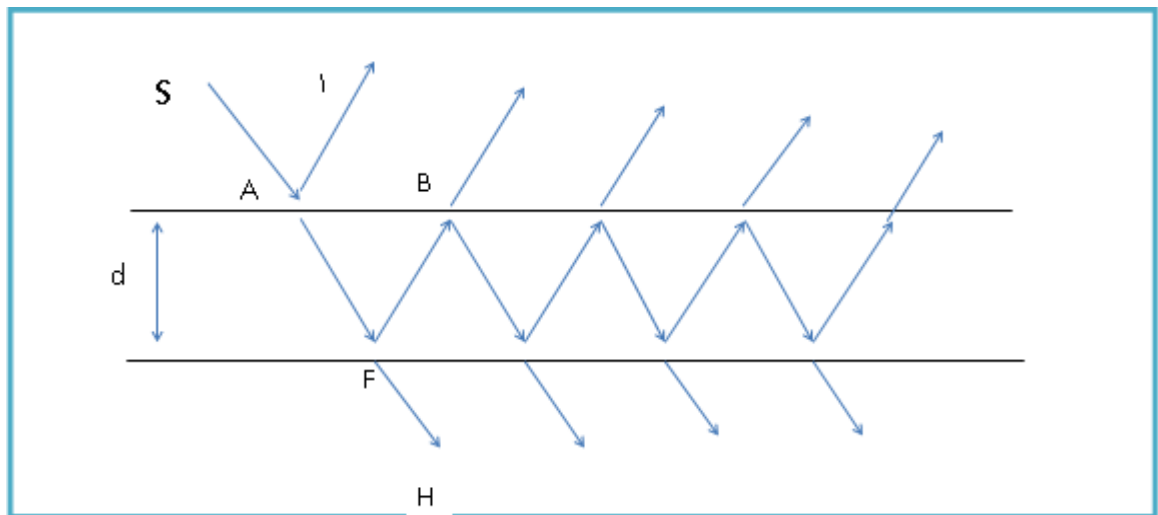
Figure (1.1): Thin-film interference at interfaces of film with geometric thickness (d) [11].

The light rays will interfere in either distractive or constrictive interference on the interface between the incidents and reflected after many internal reflections inside the film with physical path (d). The condition of distractive and constrictive interference are:

$$\delta = 2\pi/\lambda \,.\, nd \tag{1-1}$$

$$nd = \lambda/4 \tag{1-2}$$

$$\delta = \pi/2$$

$$d \sin \theta = (n + 1/2)\, \lambda \quad [14]. \tag{1-3}$$

where n represents of Refractive index , δ represents the Angle phase difference.

The speed of propagation of electromagnetic wave in material mediums is determined by nodular refraction coefficient (N) [14] :

$$N = n - ik \qquad (1\text{-}4)$$

where n represents the real part of refractive index N

k represents the extinction coefficient which is the imaginary part of N , and is connected to absorption coefficient (α) by the relation :

$$\alpha = 4\pi k / \lambda \qquad (1\text{-}5)$$

where λ is the wavelength of the incident light

1.4 Types of Antireflective Coatings (ARCₛ)

The main principle of the thin-film optical coating's is based on the constructive and destructive interference principle between the light rays emerging from thin-film coating after suffering multiple internal reflections in the interfaces of these layers [7]. ARCₛ classified into several types according to:

Firstly, Number of Layer used into:

a- Single layer, b- Double layer, c- Multilayer

As shown in Figure (1-2)
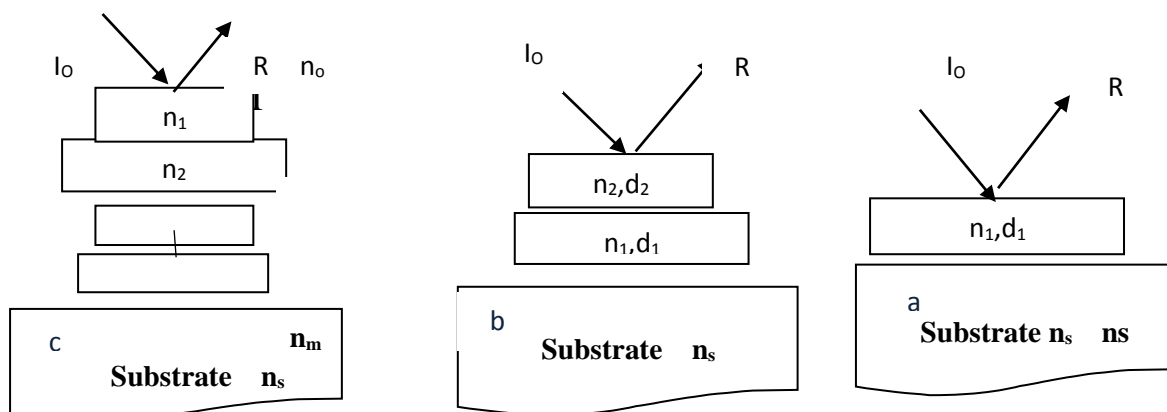
Figure (1.2) the system of antireflection layer (ARCₛ) of a- Single layer b- Double layer c- Multi layer [8].

where …n_1 ,n_2 …,d_1 , d_2 … refractive indices and geometric thicknesses of layers, respectively.

Secondly, Optical performance : which As the reflectance or transmittance or absorbance is a function of the wavelength or frequency so it is defined according to the following optical per formant:

    a- **V-type** : Where the reflectance equal zero at the design wavelength λ_o [15].

    b- **W-type** : This type is characterized by the presence of two regions of the spectrum where the reflectance equal zero , and in the middle a narrow area where the reflectivity is equal to the reflectivity of the substrate [15,16].

    c- **U-type**:   Where the reflectivity equals zero at a specific range of wavelengths [10].

    d- **Extended U-type** : Where the reflectivity equals zero at a wide range of wavelengths [10].

    e- **π-type** : This type is designed to operate at two specific wavelengths at the same time , where reflectivity equals zero at these two wavelengths and is high at other wavelengths[17].

    Each one of these types has it's specific use for instance : V-type is used in LASER systems specifically at the Nd:YAG wavelength, [18] while W-type is used in the same LASER systems but at two wavelengths that are very close to each other . These types of ARC$_S$ according to its optical performance is show in Figure (1.3).
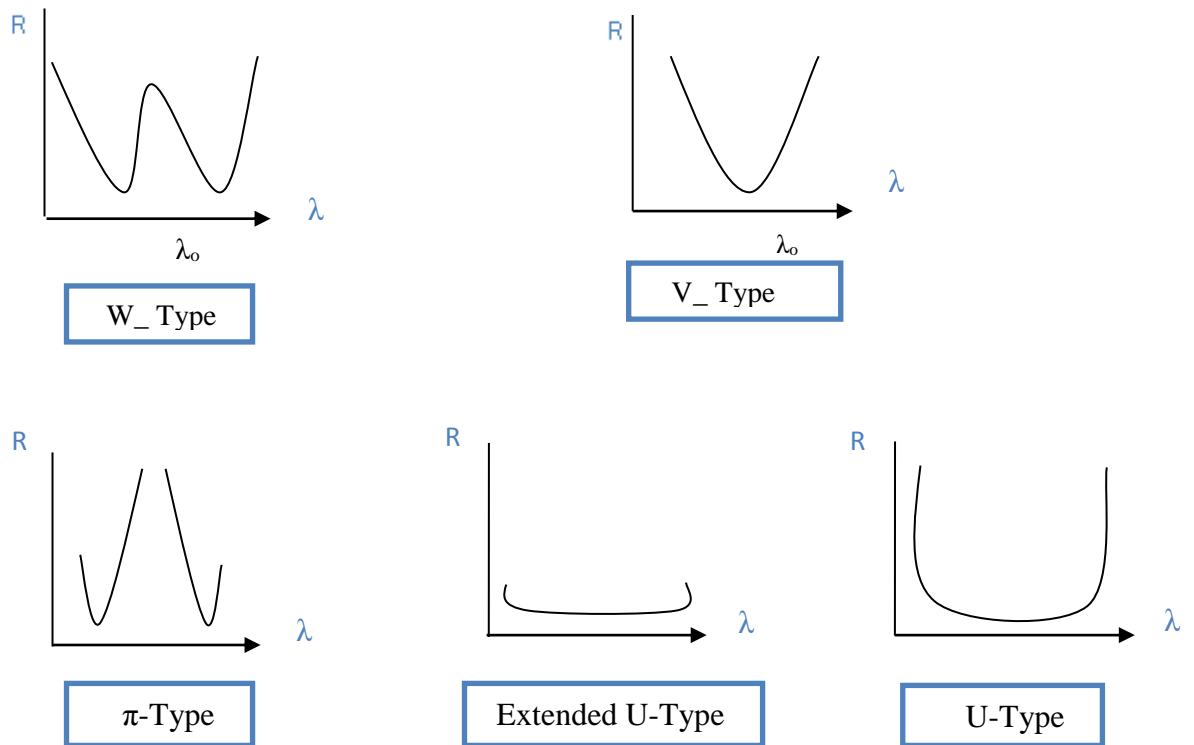
Figure (1.3)

Types of ARC$_S$ according to its optical performance [18].

Thirdly: Substrates refractive index which is divided in to: **a-Low-refractive index substrate;** In this type the coating is precipitated on a substrate of low refractive index which used to study the spectrum distribution in the visible region and the near-infrared region, such as BK-7 glass [(n$_s$ = 1.52) at a design wavelength (λ_0 =550 nm)] [11].

   b-High – refractive index substrate; In this type the coating is precipitated on a substrate of high refractive index which used to study the spectrum distribution in the infrared region of the electromagnetic spectrum , such as Germanium (Ge) [(n$_s$ = 4.0) at design wavelength (λ_0 = 2.3 μm)] and Silicon (Si) [(n$_s$ = 3.42) at design wavelength (λ_0 =1.7 μm)] [19].

1.5 ZnO Structure

Zinc oxide (ZnO) is a wide-bandgap semiconductor of the II-VI semiconductor group. polar hexagonal structure; the c axis is parallel to z axis and has prefer orientation of (0002). In almost ZnO, zinc atoms arrangement in hexagonal close packing (hcp). While, the oxygen atom have tetrahedral structure surrounding by four zinc atoms as shown in Figure 1.4.The two lattice parameters, a and c of hexagonal unit cell in wurtzite structure with ratio of c/a=1.633 and belongs to the space group of P63mc - C46v are= (0.3296 and c = 0.52065 nm) [20].
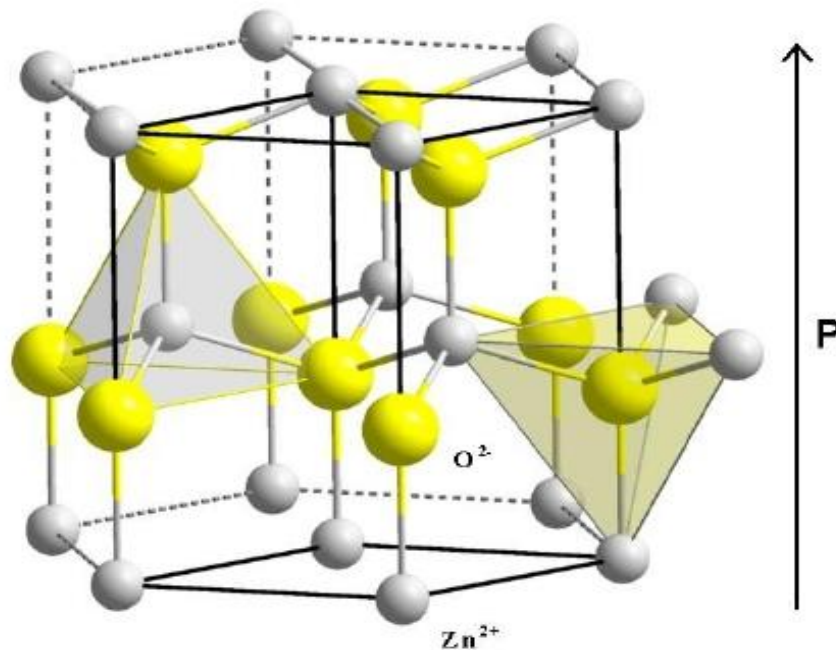
Figure (1.4): The wurtzite lattice of ZnO: small circles represent zinc atoms, whereas large circles depict oxygen atoms [20].

Table (1.1): shown the properties of bulk wurtzite lattice structure of ZnO [20].

Property	Value
Lattice parameter	a= b=3.25 A$^{\circ}$ c= 5.21 A$^{\circ}$ u= 0.348 c/a= 1.593-1.6035
Density	5.606 gm/cm^3
Melting point	2248 K
Stable crystal structure	Wurtzite
Dielectric constant	8.66
Refractive index	2.008
Band gap (Eg)	3.37 eV,(direct)
Exciton binding energy	60 me V
Electron/ Hole effective mass	0.24 $m_{\circ}$/0.59 $m_{\circ}$
Hole mobility (300) K	5-50 cm^3/Vs
Electron mobility (300) K	100-200 cm^2/ Vs

1.6 Method of Thin Film Growth Technique

There are different methods to growth the thin film, in present work ZnO films have been prepared using chemical process spin coating (sol gel) and physical process pulse laser ablation (PLA) techniques [21]. These techniques are planned in Figure (1.5) as method of thin film deposition.
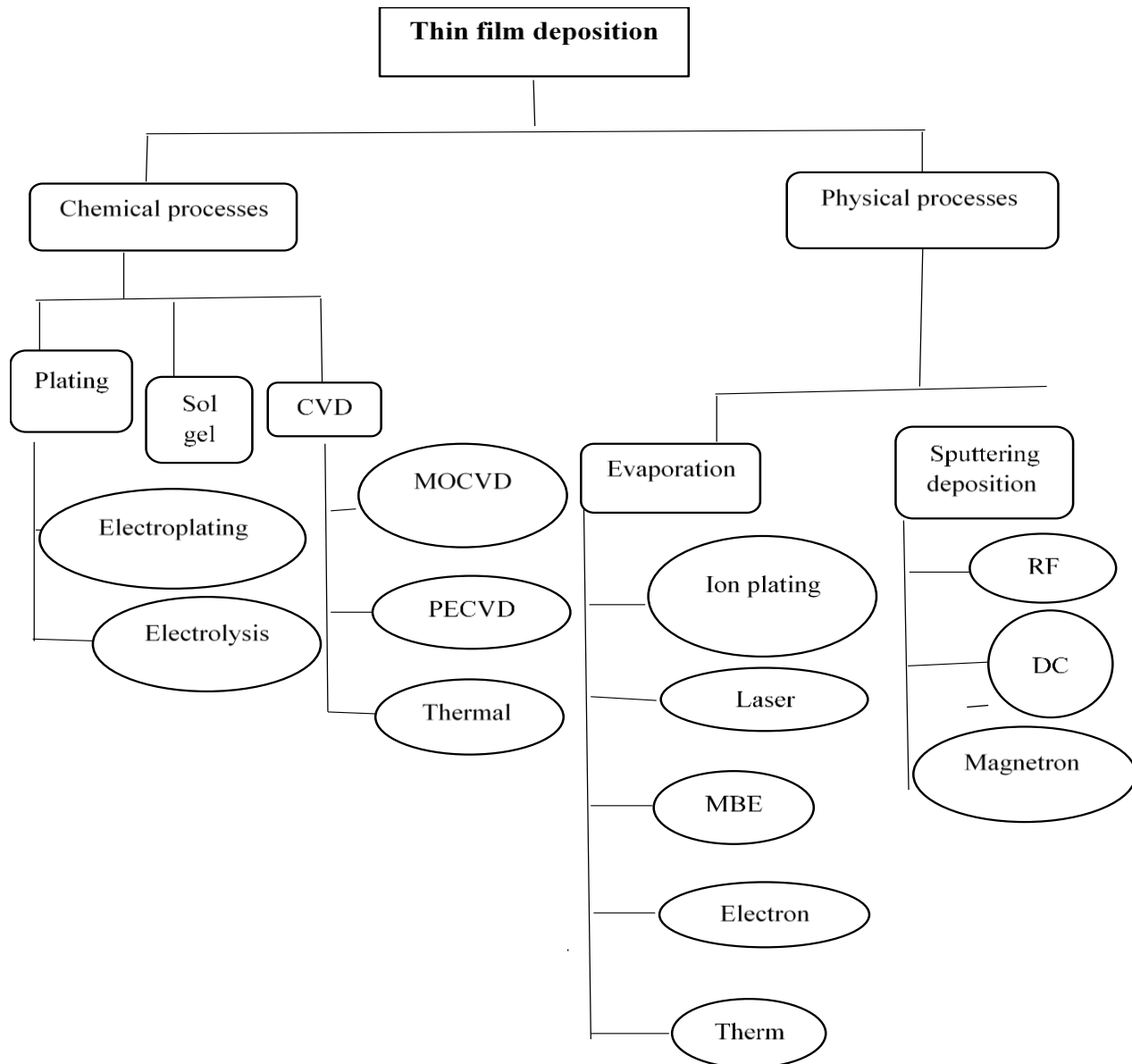
Figure (1.5): planned of thin film deposition techniques [21].

1.7 Literature Review

There are many studied in regard with design and fabrication of ZnO thin film. The reviews the ZnO materials properties and the relevant research's on the structural and optical properties of ZnO films and its associated preparation techniques have been reported.

Two techniques were used throughout the study to fabricate ZnO thin films. The techniques include the PLA, and sol-gel.as fallows:

Firstly, review on prepared ZnO thin film using PLA techniques are studied, **In 2001, Singh et al.** prepared highly conductive and transparent Al-doped zinc oxide (ZnO:Al) thin films by (PLA) technique with irradiation time of 10-60 min (6000-36000 laser shots)[22]. Then, i**n 2006, Ishikawa, et al.** successfully, produced zinc oxide nanorods using (PLA) in deionized water media at high temperature and at room temperature[23]. In addition, **Chen and Zhang** Prepared Nano-ZnO thin film by PLA and studied different factors that effect on the prepared films. Besides[24], i**n 2007, Thareja and Shukla** formatted colloidal suspension of zinc oxide nanoparticles by (PLA) of a zinc metal target at room temperature in different liquid environment[25]. **In 2008, Ajimsha et al.** prepared ZnO quantum dots (QDs) in various liquid media using LP-PLA without using any surfactant. They concluded that, the emission wavelength was tuned due to the defect and varying in the laser fluency. After that [26], i**n 2009, Cho et al.** produced ZnO Nanoparticles by (PLA) in deionized water. They revealed that there are strong in fluency of parameters such as, laser power, ablation time, and aging[27]. **In 2010, Virt, et al. s**tudied the properties of ZnO and ZnMnO thin films prepared by (PLA) that have polycrystalline behavior with average sizes of particles of ZnMnO film at 300 K and at 473 K were 50 Å and 400 Å, respectively [28]. **In 2011, Raid, et al.** synthesized ZnO by (PLA) in double distilled water with various laser fluencies at RT. They founded that, the optical properties, size, and the morphology of prepared ZnO have influenced by laser fluency and wavelength [29]. **In 2012, Atanasova, et al**. prepared of ZnO nanostructure by (PLA) and some changes occurring on the surface of the films after continued exposure in air [30]. **In 2013, Nakamura, et al**. succeeded in synthesized ZnO nanoparticle by (PLA) method by Q-switched Nd:YAG laser in the air with spheres shape of diameters 10-20 μm [31]. **In 2015, Fadhil and**

Hadi prepared zinc oxide nanoparticles by (PLA) of in isopropanol at room temperature at different laser fluency [32]. **In 2016, Salim et al.** fabricated ZnO Nanoparticles using LP-PLA system at a different laser wavelength (1.06 and 0.532µm), laser fluency and number of the laser pulse. They studied the effect of these parameters on surface morphology and found that the grain size of the films increased with laser fluency and decreased with number of laser pulses [33]. **In 2016, Farahan, et al**. prepared ZnO nanoparticles by (PLA) and studied the effect of solvents (methanol and distilled water) on the characterization of ZnO. They found that the ZnO nanoparticles have a hexagonal crystal structure and different size was formed due to the change of environment of laser pulse. Additionally [34]. **Ismail, et al.** synthesized of pure and Er+3 doped ZnO nanoparticles by using (PLA) in ethanol at room temperature and found that the surface in granular morphology [35]. Late, i**n 2017, Khashan and Mahdi**. Synthesized ZnO: Mg nanocomposite by (PLA) in liquid and they found that, the sample has hexagonal wurtzite [36].

In addition, the sol-gel technique is important method in the preparation of ZnO films, and several studies have focused on this method. These studies belong the sol –gel technique to proper, ZnO thin film is summarized below as following:-

The use of sol-gel chemistry started in 1956. The first scholar who worked on it was Rustom Roy, a graduate student working under Elburt F. Osborn. Roy used sol-gel chemistry to synthesize composites of tetraethoxide and metal nitrate salts for phase equilibrium studies.

 In 2001, Phani, et al. investigated the synthesis and characterization of AZO thin films prepared by the sol-gel technique. The AFM and SEM images reveal uniform, continuous, homogeneous films. XPS analysis showed 17% Zn, 14% Al, and 60% O in the film treated at 700 °C for 5 h. The formation of 800 °C/5 h annealed films indicated the

stoichiometric formation of $ZnAl_2O_4$ [37].Then, **in 2007, Murali.** examined the properties of sol-gel dip-coated ZnO thin films. The optical absorption measurements of band gap energy ranged from 3.17 eV to 3.32 eV. The resistivity of the films ranged from 1000 to 10 000 Ω cm. He showed that the resistivity can be decreased by doping impurities such as Ga, Al, Mn, etc [38]. In addition, **in 2007, Xiaofeng et al.** used a humidity sensor based on a quartz tuning fork (QTF) and the sensor coated with a sol-gel-derived nanocrystalline thin film. The QTF coated with sol-gel-derived nanocrystalline ZnO thin film made high sensitive and rapid detection of water vapor, and they found that the uniformity of the ZnO film is also important in the sensitivity of the sensors [39]. Besides, **in 2007, Bhattacharyya et al.** studied the fast response of a methane sensor using nanocrystalline ZnO thin films derived from the sol-gel method. The thin nanocrystalline ZnO films produced by the well-known sol-gel method produce an efficient resistive gas sensor for sensing methane [40]. After that, **in 2009 Mehmet et al.** conducted sol-gel synthesis studies, comparative characterizations, and reliability analyses of undoped and Al-doped ZnO thin films. The thin films of sol-gel derived undoped and Al-doped ZnO material systems are fabricated for transparent conducting oxide modules. The results of both temperature cycling and accelerated delamination tests demonstrated a high physical reliability [41].Then, **in 2011 Jagadish and Pearton.** investigated the influence of the annealing temperature on the structural, topographical, and optical properties of sol-gel derived from thin ZnO films, they conclude that the crystallinity, degree of preferred orientation, and average grain size of the films increase with the annealing temperature. The annealed ZnO films also showed good transparency within the wavelength region of 400–800 nm [42]. And aging, **in 2011 Shane et al.** examined the effect of doping on the

morphology, microstructure and electrical properties of transparent ZnO films prepared by the sol-gel method. The minimum doping concentration was 2% throughout the study and Aluminum (Al) is required to produce more conductive materials need to observe by sheet resistance measurements. These measurements are susceptible to variation depending on the annealing temperature. In terms of the electrical properties of the films, the porous undoped ZnO films were highly resistive and the AZO films were have a significantly lower sheet resistance [43]. Also, **in 2011 Sathya et al**. studied thin films from a fair share in the ever growing solar cell research and also in the market. One of the most versatile materials grown as thin films today are from derivatives of pure and doped Zinc Oxide .A combination of dip coating and electrodeposition is a powerful tool in order to achieve good quality thin films. The main advantage is that the basic precursor which is Indium Tin Oxide (ITO) can be safely avoided since its procurement enhances the cost and the availability if selective nowadays [44]. **In 2012 Yang et al.** studied the structure, morphology, and electrical characterization of DC-sputtered ZnO thin films. The study revealed that the grain size increased because of its low boundary scattering. This attribute increases the value of the surface roughness and the variations in electrical conductivit [45]. In addition, **in 2014 Yarub Al-Douri et al.** studied the structural and optical properties of indium (In) doping in zinc oxide (ZnO) using chemical spray deposition technique, they showed that X-ray diffraction (XRD) peaks observed a change in preferential orientation from (002) to (101) crystal plane with increasing in In dopant concentration [46]. Then, **In 2016, Alaa. Ghazai, et al**. synthesized pure zinc oxide (ZnO) and Al-doped ZnO thin films by sol gel method. They found that the films have polycrystalline hexagonal wurtzite structure and the lattice constants, crystallite size and strain decreased as

the Al dopant concentration increases in ZnO lattice. In addition, band gap energy of ZnO is 3.37 eV with direct band to band transition and decreased to 3.25 eV with increased Al-doping concentration [47]. **In the same year, Alaa. Ghazai, et al.** fabricated (ZnO) thin film by sol gel method with different zinc acitate to MEA ratio. XRD results showed that the prepared films have a polycrystalline in nature. The referred orientation ZnO (002) has the lower grain size to be 9.9 and 8.3 nm for zinc acetate. SEM images are in agreement with the XRD results that films with zinc acetate have a rough surface [48].

1.8 Aim of the work

The objectives of this work are to fabricate a nanostructure ZnO thin film on glass and p Si using PLA and sol gel techniques. The prepared films have been characterized to study the structural and optical properties using XRD, SEM, EDX and UV-Vis spectroscopy. As well as, the effect of pulse, types of solvent, types of substrate and energy on the structural and optical properties studied.

1.9 Outline of the work

This thesis consists of five chapters. Chapter one provides a background of ZnO thin film, the methods of fabricating ZnO thin film and reviews the relevant literature about ZnO thin films. Chapter tow presents the theoretical part of the work. Chapter three present the methodologe of research and the general description of the equipment used the experimental section also characterizes the preparation of ZnO thin film. Chapter four presents and discusses the analysis results of the properties of the fabricated ZnO film deposited on glass substrate. Chapter five presents conclusions and suggestions for future research.

Chapter Two

Theoretical part

2.1 Introduction

This chapter includes a general description of the theoretical part of the present study and physical concepts that related to the calculated parameters.The laser beam parameters including wavelengh of laser used to prepare the samples, pulse laser duration, energy and peak power density have been stated . In addition, the calculation of the crystal structure parameters such as lattice constant, crystalline size, FWHM, dislocation density and microstrain have also been discussed.

2.2 The Characteristic Matrix of Single Thin Film

The state of excitation in a vacuum caused by electric charge, which known as an electromagnetic field, which represents the electric field vector E (electric vector) and magnetic induction vector $\bar{H}$. To study the interaction of electromagnetic radiation with material that the satisfy Maxwell's equation, depend on the solution of Maxwell's equations, of homogeneous and isotropic medium [49].

The single thin film component from two interval boundary (a and b) as show in Figure (2.4) the plane wave incident on a thin film [15].

Incident plane
Wave front

Boundary a

d   Physical thickness of film n_1 Thin film

Normal to film boundaries   Boundary b

Z
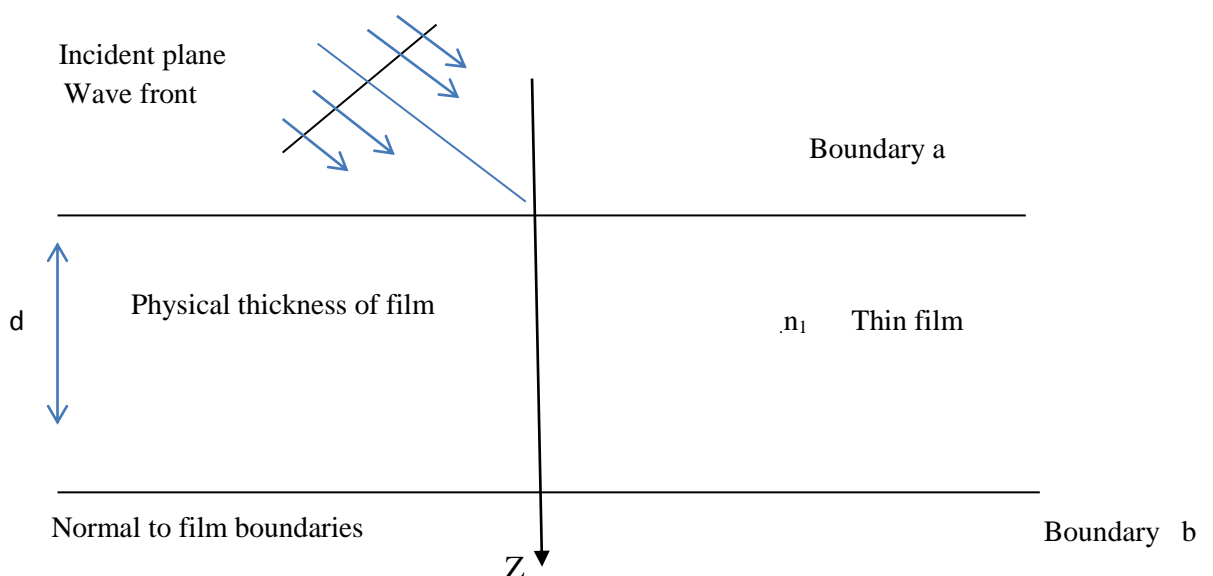
Figure (2.1): Plane wave falling on the thin film [58].

n_s Substrate

The incident light at the interval boundary (a) will reflect and the penetrating part from it will reflect at the interval boundary (b). Symbolized to the incident wave with symbol (+) and the reflecting wave with symbol (-); By applied the boundary condition of the Maxwell equations, and suppose that the material is non-magnetic (i.e $\sqrt{\varepsilon_\circ \mu_\circ} = 1$) the components of the electric and magnetic fields at the the two interval boundary a, b respectively are [15]:-

$$E_b = E_{b+} + E_{b-} \qquad\qquad (2\text{-}18)$$

$$H_b = n_1 E_{b+} - n_1 E_{b-} \qquad\qquad (2\text{-}19)$$

where the phase coefficients are neglected. By adding the two above, the incident and reflected part of the electric and magnetic wave at b boundary are.

$$E_{b+} = 1/2\ (H_b\ /\ n_1\ + E_b) \qquad\qquad (2\text{-}20)$$

$$E_{b-} = 1/2\ (\text{-}H_b\ /\ n_1\ + E_b) \qquad\qquad (2\text{-}21)$$

$$H_{b+} = n_1 E_{b+} = 1/2\ (H_b\ +\ n_1\ E_b) \qquad\qquad (2\text{-}22)$$

$$H_{b-} = \text{-}\ n_1\ E_{b-} = 1/2\ (H_b\ \text{-}\ n_1\ E_b) \qquad\qquad (2\text{-}23)$$

These field's at the interval boundary a are similar to the field's at the interval b multiply with the phase coefficient equal ($e^{i\delta}$) with relating to the incident wave and ($e^{-i\delta}$) to the reflected wave , where :-

$$\delta = 2\pi n_1 d\ /\ \lambda \qquad\qquad (2\text{-}24)$$

So, the equations become with the follow form:-

$$E_{a+} = E_{b+}\ e^{-i\delta}\ = 1/2\ (H_b\ /\ n_1\ + E_b)\ e^{i\delta}$$

$$E_{a-} = E_{b-}\ e^{-i\delta}\ = 1/2\ (\text{-}H_b\ /\ n_1\ + E_b) e^{-i\delta}$$

$$H_{a+} = H_{b+}\ e^{i\delta}\ = 1/2\ (H_b\ +\ n_1\ E_b)\ e^{i\delta}$$

$$H_{a-} = H_{b-}\ e^{i\delta}\ 1/2\ (H_b\ \text{-}\ n_1\ E_b) e^{-i\delta}$$

and the average at the boundary a as following :-

$$E_a = E_{a+} + E_b = E_b \left(\frac{e^{i\delta} - e^{-i\delta}}{2} \right) + H_b \left(\frac{e^{i\delta} - e^{-i\delta}}{2n_1} \right) \tag{2-25}$$

$$E_a = E_b \cos\delta + H_b \sin \delta / n_1$$

$$H_a = H_{a+} + H_b = E_b n_1 \left(\frac{e^{i\delta} - e^{-i\delta}}{2} \right) + H_b \left(\frac{e^{i\delta} - e^{-i\delta}}{2} \right) \tag{2-26}$$

$$H_a = i E_b n_1 \sin \delta + H_b \cos \delta$$

The two equation (2-25) (2-26) written with the matrix formula

$$\begin{bmatrix} E_a \\ H_b \end{bmatrix} = \begin{bmatrix} \cos \delta_1 & i \sin \delta_1 / n_1 \\ i n_1 \sin \delta_1 & \cos \delta_1 \end{bmatrix} \tag{2-27}$$

The equation (2-27) associated between the continue tangent components to each from the field's $\vec{E}$ and $\vec{H}$ incident on the system and the outside from it. The right side of the equation define as the characteristic matrix [50] .

The input optical admittance could express as following [51].

$$Y = \frac{H_a}{E_a} \tag{2-28}$$

and we can compute the reflecting coefficient of the film as follow :-

$$r = \frac{n_o - Y}{n_o + Y} \quad , \quad r^0 = \left(\frac{n_o - Y}{n_o + Y} \right)^0$$

$$R = rr^o = |r|^2$$

$$R = \left(\frac{n_o - Y}{n_o + Y} \right) \left(\frac{n_o - Y}{n_o + Y} \right)^o \tag{2-29}$$

And could re- writing the eq. (2-27) as follow :-

$$E_a \begin{bmatrix} 1 \\ y \end{bmatrix} = \begin{bmatrix} \cos \delta_1 & i \sin \delta_1 / n_1 \\ i n_1 \sin \delta_1 & \cos \delta_1 \end{bmatrix} \begin{bmatrix} 1 \\ n_s \end{bmatrix}$$

And

$$\begin{bmatrix} B \\ C \end{bmatrix} = \begin{bmatrix} \cos \delta_1 & i \sin \delta_1 / n_1 \\ i n_1 \sin \delta_1 & \cos \delta_1 \end{bmatrix} \begin{bmatrix} 1 \\ n_s \end{bmatrix}$$

Where $Y = C/B$ and which describe the completely system . by using this matrix for the coated substrate with film of reflection index n the eq (2-29) show the reflection of a coated film on substrate, and to found the refleative index of this film which satisfy zero reflection condition as following:-

$$R = \left(\frac{n_o n_s - n_1^2}{n_o n_s + n_1^2} \right)^2 \qquad \text{coated film} \qquad \textbf{(2-30)}$$

if R=0

so,

$n_0 n_s - n_1^2 = 0$

$n_1^2 = n_0 n_s$

$n_1 = \sqrt{n_0 n_s}$ $\qquad\qquad\qquad\qquad\qquad\qquad\qquad$ **(2-31)**

2.3 Pulse Laser Ablation in Liquids

Pulsed laser ablation in liquid media (PLAL) is a promising top-down technique for controlling the fabrication of nanomaterials through rapid reactive quenching of ablated species at the interface between plasma and liquid. PLAL is a simple method used to deposit a wide range of materials such as noble metals, alloys, oxides and semiconductors. It is simple and free from limitations because it can generate nanoparticles without counter-ions or surface-active substances. It is consider a high-power pulsed laser beam irradiates on a metal target in a transparent liquid and produce a local plasma, with super high temperature (about 6000 K) and high pressure on the solid-liquid interface. This quench

quickly after one pulse due to adiabatic expansion of the plasma and its interaction with surrounding media [52]. This technique of pulsed laser ablation and deposition is shown in Figure (1.6).
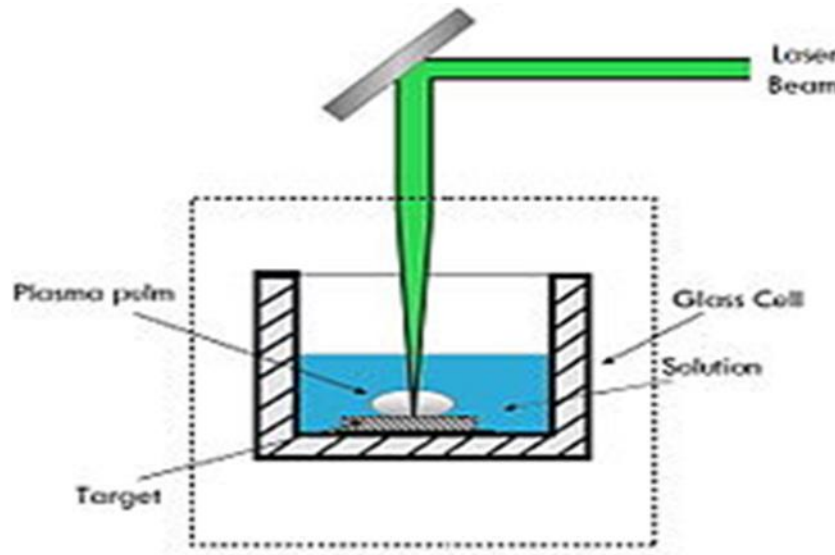
Figure (2.2): Laser ablation in Solution technique [22].

2.3.1 The Advantage of The Pulse Laser Ablation in Liquid (PLAL) Technique

There are many advantage of the PLAL technique can listed as follows:

1-Simple and clean well-crystallized (NPs) to the convention techniques [53].

2-Preparing metal colloids with absence of chemical reagents in solutions. Therefore, pure colloids, which will be useful for further applications, can be produced [24.[

3-Easy to automate and not need to the extreme temperature and pressure [53].

4-Resizing and reshaping are also possible through melting and fragmentation technique [54].

5 -The solvent can provide (i) physical effects such as confinement and cooling, (ii) chemical effects such as oxidation and size controlling, and (iii) coating effect to prevent particle size increase [55].

6-There is a possibility to prepare various kinds of nanoparticles such as: metals, semiconductors, oxides, hetero structures and core–shell NS [56].

2.4 Laser Beam Parameters

The beam of electromagnetic radiation is presented the energy of laser. When the laser beam is incident on the selective substrate will be react with it. There are many important parameters which the laser performance depend on it such as, wavelength of laser used, pulse duration or laser ablation time duration, number of laser pulses energy and peak power, the solvent kind of the substrate and beam focusing, whatever, some of these parameters will discussed in the following subsections which including in this work [57].

2.4.1 Wavelength of Laser Used

The wavelength of laser radiation used is depend on the active region or meduim of the laser. It is visible of (ruby, He-Ne) laser and invisible of (Nd:YAG) laser. Table (2.1) show the wavelength values of some lasers [58].

Table (2.1): Wavelength values of some lasers and its active region [58].

Type	Wavelength (µm)
Carbon dioxide	10.6
Carbon monoxide	5.4
Nd-YAG	1.06
Nd-glass	1.06
Excimer	0.249

The wavelength of the laser used is related with the reflectivity of the metal which employed with laser system. In general, the reflectance increases with the increasing of the wavelength which the lasers with wavelength [54].

2.4.2 Pulse Laser Duration

Since all lasers should be broad line extremely monochromatic to produce pulses of very short duration lasers, such as solid-state and liquid lasers [65]. These propertly offer an advantages in compare with the conventional sources, which start with its ability to ablate an atomic in material in a very short time period and thermal diffusion is occured. After the electron in atoms are absorbed the laser energy, the electron temperatures reached to be more than thousands of Kelvin degrees and these energy transfer from the electrons to the atomic lattice, caused material removal, ablation, and plasma have been occured. This processing as well as, thermal relaxation is governed by the thermal diffusion length (L_t) and thermal wave can propagate during the laser pulse which related to the laser pulse width (t_p) as following [59]:

$$L = \sqrt{D^t}\, p \qquad\qquad\qquad (2\text{-}30)$$

where D is the thermal diffusivity of the material [60]. Figure (2.3) shows the effect of laser pulse durationn on metal depth.

Figure (2.3): Effectof laser pulse duration on metal depth [60].

2.5 Spin Coating (Sol gel) Parameters

Spin coating is one of the most common techniques for preparing of thin films on substrates and it is used in a wide industries and technology application. The advantages of spin coating method are the ability to produce uniform films from a few nanometres to a few microns in thickness quickly and easily. in addition it is simpilicty and cheap in compare with other method, There are many parameter related with this method such as the solution concentration the number of rotation per minte (rpm) and interval time have been included in this work.While, the disadvantage is an inherently batch (single substrate) process and therefore relatively low throughput compared to roll-to-roll processes. The fast drying times can also lead to lower performance for some particular nanotechnologies, which require time to self-assemble and/or crystalline. Finally, the material usage is typically very low at around 10% or less with the rest being flung off the side and wasted. Whilst this

is not usually, an issue for research environments it is clearly wasteful for manufacturing [61].

2.6 Structure parameters Analyses

There are many instruments have been used to characterize the Structural properties of thin film under study, such as X ray diffraction (XRD),Scanning electron microscobe (SEM), and energy dispersive X-ray (EDX) as following:

2.6.1 X-Ray Diffraction (XRD) and Parameters Calculation

Normally XRD is used to calculate different parameters which could be used to clarify the studies of the deposited films. In addition, very useful and widely used technique for characterizing solid materials is X-ray diffraction (XRD).The technique reveals detailed information about the chemical composition, crystallographic structure, orientation and various defects in a crystalline material. The process of interaction between X-rays and the electrons in a matter are governed by inelastic scattering and give rise to Compton scattering or elastic scattering through Thomson scattering [62]

2.6.1.1 Lattice Constant (a)

Lattice Constant (a) can be calculated of a particular cubic system through the following relation [63]:

$$d_{hkl} = \frac{a}{\sqrt{h^2+k^2+l^2}} \qquad (2\text{-}36)$$

and of hexagonal system

$$d_{hkl} = \frac{1}{\sqrt{4\backslash 3(h^2 + hk + k^2)\backslash a^2 + l^2 \backslash c^2}} \qquad (2\text{-}37)$$

2.6.1.2 Averge crystalline size

The crystalline size in a nanomaterial can be determined using the X-ray data and applying the Scherrer equation [64]:

$$D = k\lambda/\beta\cos\theta \qquad (2\text{-}38)$$

where D is the crystallite size, λ is the x-ray wavelength ($\lambda = 0.14506$ nm), β is the line broadening at FWHM (full width at half maximum intensity), θ is the Bragg angle and K is the shape factor, when K is unknown and cannot be determined, 0.9 is used as a good estimate, the coefficient K depends on such factors such as the geometries of crystallites

2.6.1.3 Full Width at Half Maximum (FWHM) (β)

The FWHM of the preferred orientation (peak) could be measured directly from the X-ray diffraction pattern, since it is equal to the width of the line profile (in our case in radian) at the half of the maximum intensity as in Figure (2.6) [65].
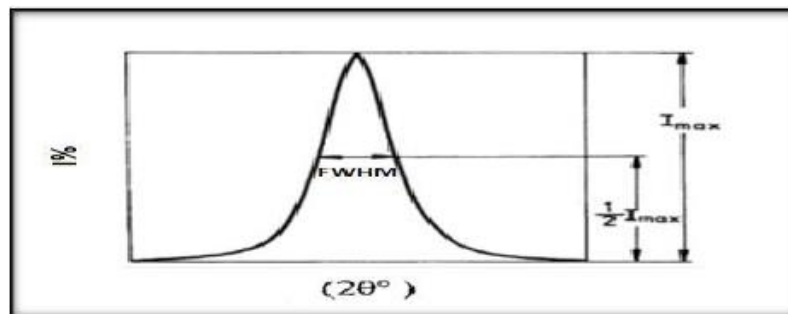
Figure. (2.4): FWHM of The Preferred Orientation of the X-Ray Diffraction Pattern [65].

2.6.1.4 Dislocations Density:

The number of dislocations in a material is defined as the dislocation density δ the total dislocation length per unit volume or the number of dislocations intersecting a unit area which are given by[67]:

$$\delta = \frac{1}{D^2} \qquad\qquad\qquad \textbf{(2-39)}$$

Crystallographic lattices are never perfect, but contain lattice faults that may be characterized by their spatial extension as zero-dimensional point defects, one-dimensional line defects or two-dimensional area defects. A dislocation causes the neighboring atoms to shift from their ideal lattice sites and thereby introduces a strain field in the surrounding volume see Figure (2.7). The strain field may extend over a distance of some micrometers from the core of the dislocation and the defect line thus affects a large volume.
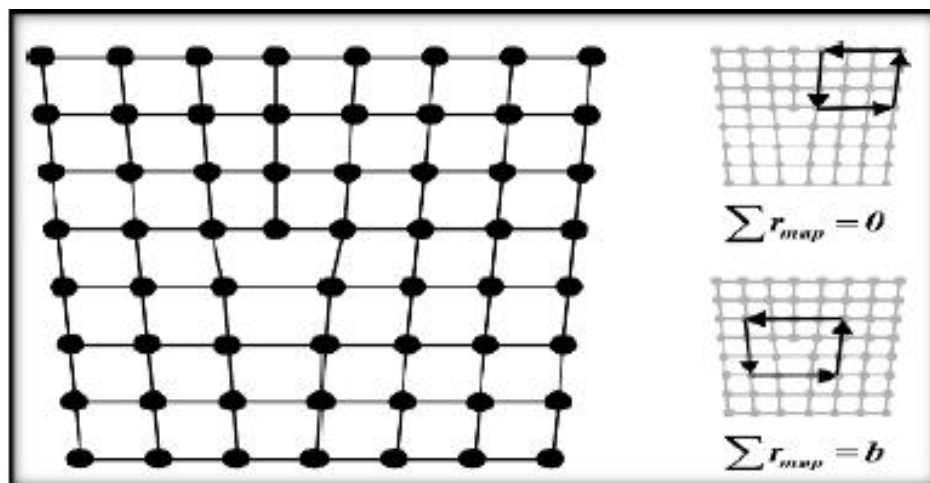
Figure. (2.5): An Edge Dislocation in a Simple Cubic Lattice[67]

2.6.1.5 Microstrain (ε)

The micro strains are caused during the growth of thin films, and will be raised from stretching or compression in the lattice to make a deviation. So the strain broadening is caused by varying displacements of the atoms with respect to their reference lattice position [68]. This strain can be calculated from the formula: [69]

$$\varepsilon = \beta \cos\theta / 4 \qquad\qquad\qquad (2\text{-}40)$$

2.6.2 Scanning Electron Microscopies

Scanning electron microscopy (SEM) which combine with Energy dispersive X-ray speectroscopy (EDX) is basically a type of electron microscope. Electrons are thermionically emitted from a tungsten or lanthanum hexa boride (LaB6) cathode which flies towards an anode; alternatively electrons can be emitted via field emission (FE). Tungsten is used because it has the highest melting point and lowest vapor pressure of all metals, thereby allowing it to be heated for electron emission. The electron beam, which typically has an energy ranging from a few hundred eV to 50 keV.

2.7 Optical Properties

The optical properties of a semiconductor are related to intrinsic effect. Based on the intrinsic location of the top of the valence band (V.B.) and bottom of the conduction band (C.B.) in the band structure Figure (2.8) the electron-hole pair generation occurs directly or indirectly. The ZnO thin film is a wide direct band gap compound semiconductor. It is highly transparent in the visible range (depends on

the deposition technique and thickness). The n-type conductivity is due to the lack of oxygen and an excess of zinc [70].
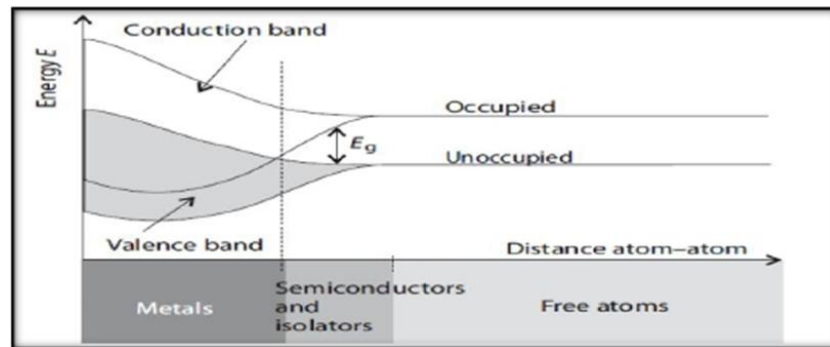
Figure :(2.6) Formation of Energy Bands in Silicon Lattice Crystal By Bringing Together Isolated Atoms [71].

2.7.1 Optical Absorption and Absorption Edge

The fundamental absorption is the most important absorption process, which involves the transition of electrons from the valence to the conduction band, which displays itself by a rapid rise in absorption, and this can be used to determine the energy gap of the semiconductor [72].

The semiconductor absorbs photon from the incident beam, the absorption depends on the photon energy (hυ), where h is Planck's constant, υ is the incident photon frequency, the absorption is associated with the electronic transition between the V.B. and the C.B. in the material starting at the absorption edge which corresponds to minimum energy difference (E_g) between the lowest minimum of the C.B. and the highest maximum of the V.B. If the photon energy (hυ) is equal or more than energy gap (E_g) then, the photon can interact with a valence electron, elevates the electron into the C.B. and creates an electron–hole . The maximum wavelength (λ_c) of the incident photon which creates the electron–hole pair is can be expressed in the following expression as [73]:

$$\lambda_c(\mu m) = \frac{hc}{E_g} = \frac{1.24}{E_g(ev)} \qquad \text{(2-41)}$$
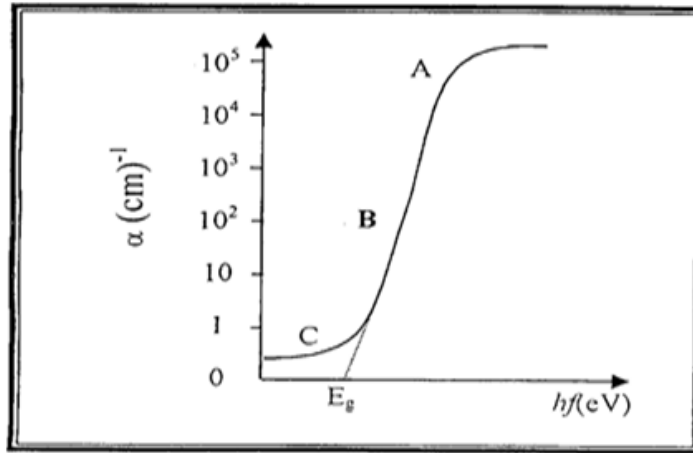
Figure. (2.7): Fundamental Absorption Edge of Crystal Semiconductor [94]

The intensity of the photon flux decreases exponentially with distance through the semiconductor according to the following equation [74].

$$I = I_\circ \exp(-\alpha d) \qquad \text{(2-42)}$$

Where $I_\circ$ and I are the incident and the transmitted photon intensity respectively and α is the absorption coefficient, which is defined as the relative number of the photons absorbed per unit distance of semiconductor, and d is the thickness of the film [75].

(α) Can also give as:

$$\alpha = 2.303 \; \frac{A}{d} \qquad \text{(2-43)}$$

Where A: represent the absorbance, d: represent is the sample thickness

2.7.2 Direct Transitions

The direct transition in general occurs between top of valence band and bottom of conduction band (vertical transition) Figure (2-10) at

the same wave vector ($\Delta k = 0$) for conservation of momentum. The allowed direct transition Figure(2-10a) refers to that transition which occurs between top of the valence band and bottom of the conduction band when the change in the wave vector equal to zero ($\Delta k = 0$).

This transition is described by the following relation [76].

$$\alpha h\nu = B(h\nu - E_g)^{1/2} \qquad\qquad \text{(2-44)}$$

Where B constant is inversely proportional to amorphusity.

hν is the photon energy.

Eg : is the band gap.

If the transition occurs between states of the same wave vector, but the wave vector does not equal to zero, the transition is called forbidden direct transition Figure (2-10b), it obeys the following relation [77]:

$$\alpha h\nu = B(h\nu - E_g)^{3/2} \qquad\qquad \text{(2-45)}$$

2.7.3 Indirect Transitions

In indirect transition there is a large momentum difference between the points to which the transition takes place in valence and conduction bands, this means that the conduction band minimal are not at the same value of K as the valence band maxima, then, assistance of a phonon is necessary to conserve the momentum, therefore:

$$h\nu = E_g \pm E_p \qquad\qquad \text{(2-46)}$$

Where E_p is the energy of an absorbed or emitted phonon. For an allowed indirect transition, the transition occurs from the top of the valence band to the bottom of the conduction band as shown in Figure (2.10c) so that [78]:

$$\alpha h\nu = B(h\nu - E_g)^2 \qquad\qquad \text{(2-47)}$$

   While, the forbidden indirect transitions occur from any point near the top of V.B. to any point other than the bottom of the C.B., as shown in Figure (2.10d).

   Experimentally it is possible to differentiate between direct and indirect processes by the level of the absorption coefficient (α); α takes values from 10^4 to 10^5 cm^{-1} for direct transitions and 10 to 10^3 cm^{-1} for indirect transitions at the absorption edge [79].
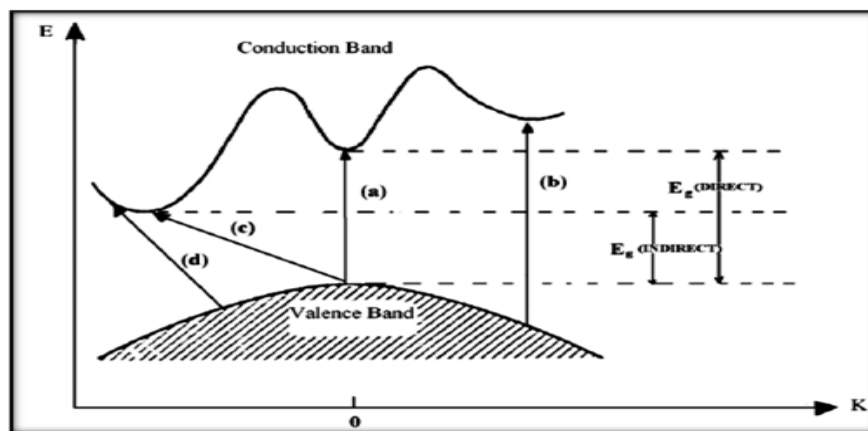
Figure (2.8) The optical transitions (a) Allowed direct, (b) Forbidden direct; (c) Allowed indirect, (d) Forbidden indirect [80].

Chapter Three

Experimental Work

3.1 Introduction

This chapter describes the experimental procedure and the basic principle of the various physical techniques used to synthesize and studying the properties of ZnO nanoparticles colloidal solution. In addition, then studying of the preparation condition of ZnO in PLA method with different liquid, and in spin coating environment. Figure (3.1) show the steps of this work.
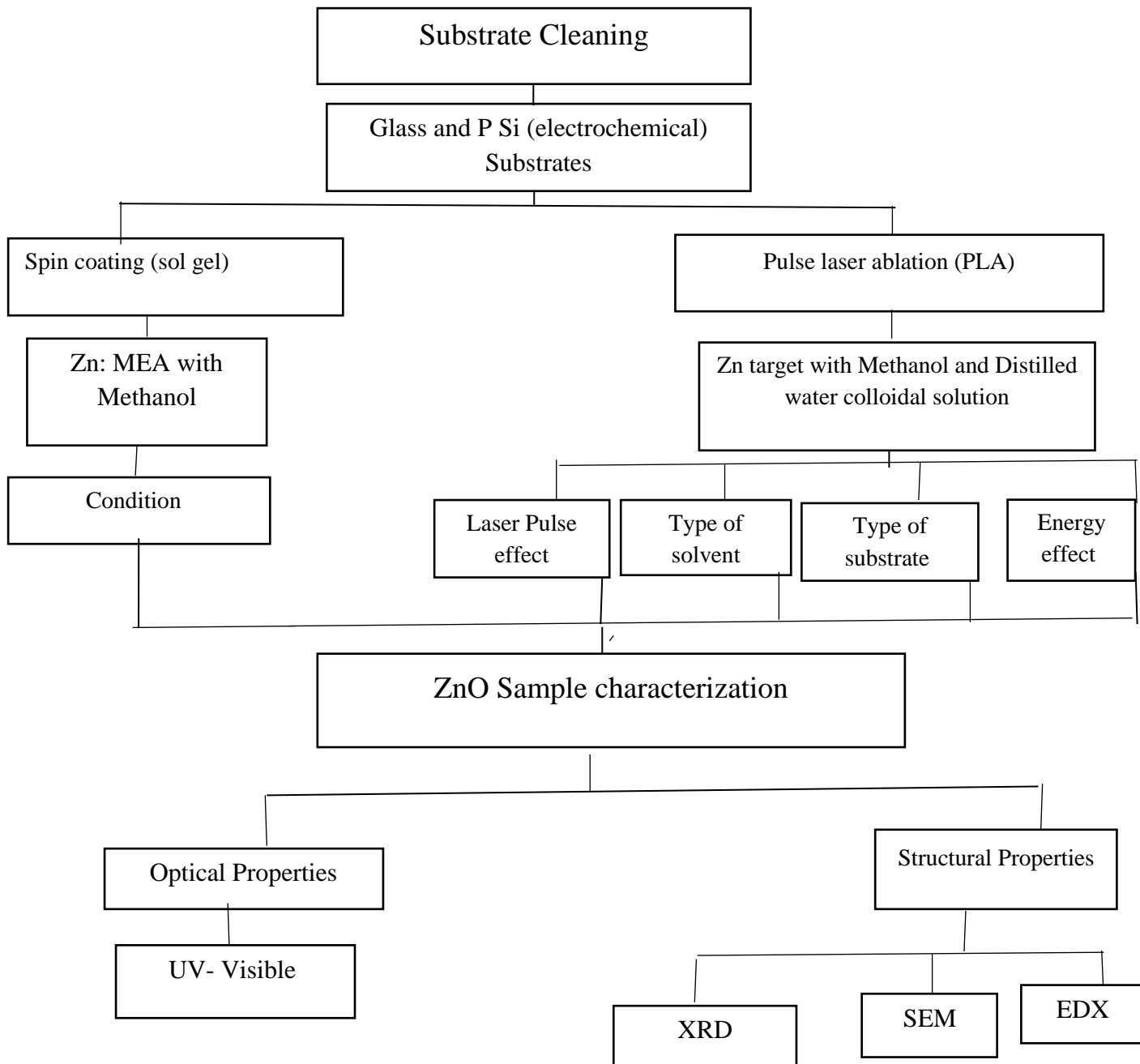
Figure (3.1):The Diagram of experiment steps of research under studying.

3.2 Substrates Preparation and Cleaning

In present work, glass and porous silicon have been used as a substrate, The description of the preparation of these substrates will be mention more details in the next two section.

3.2.1 Glass Substrate

Glass substrate is used to deposit ZnO thin films with dimensions (2.5×2.5) cm^2.The cleaning of the substrate is very important because it has a great effect on the properties of the films. The process can be summarized by the following steps:

1. Using tap water to remove any dust that might be on the surface of the substrates and then placed them in distilled water for 60 minutes.

2.   Immersing the substrates in a pure acetone solution, which reacts with contamination such as grease and some oxides, this process, is fulfilled accurately by rewashing the substrates in the ultrasonic bath for 10 minutes.

3. Drying the slides by wiping them with soft paper.

3.2.2 Porous Silicon(PSi) Substrates

The silicon wafer was n-type (111) orientation with $(1.5\text{-}4)$ Ω.cm resistivity and $(300 \pm 15$ µm) thickness. cut to Square-shaped of single crystal silicon substrates, each of (1x1) cm^2 area. The silicon (Si) samples were cleaned by Radio cooperation of America (RCA) and then by alcohol with ultrasonic bath in order to remove the impurities and residuals and to remove the native oxide from their surface. in order to make porous silicon substrate,

electrochemical etching method (ECE) has been used. The electrochemical etching cell is the important part of the fabrication system as the homogeneity of Pours silicon (PSi) samples depends on its structure. The electrochemical etching ECE cell, used in this work, is schematically in Figure (3.2).

-a-   -b-
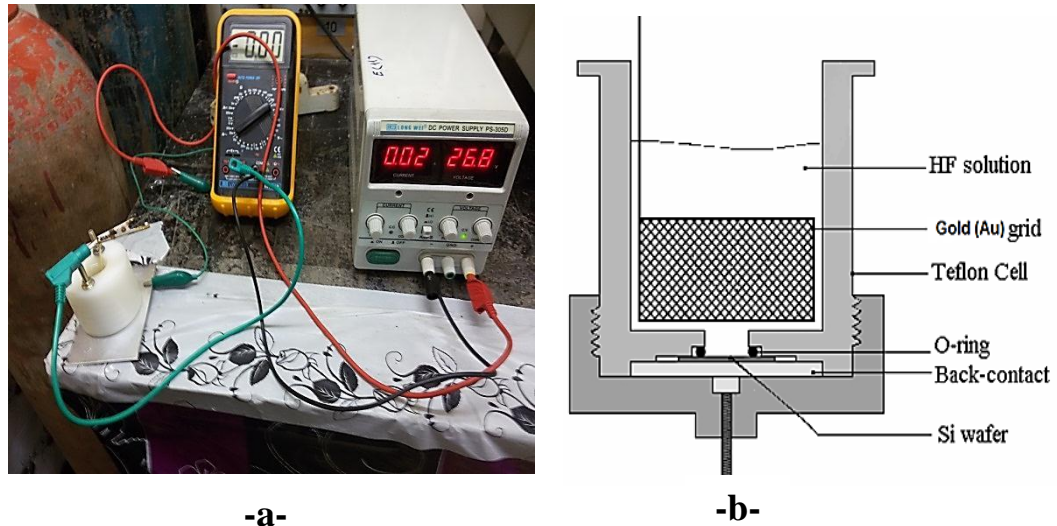
Figure (3.2): (a) Schematic of porous silicon set-up (b) the electrochemical etching cell.

The PSi formed under conditions 30 min of time with 1:3 mixture of HF concentration 50% with ethanol and current densities 20–25 mA/cm^2. All these requirements were considered as effective parameters in the ECE process.

3.3 Zn Target and Colloidal Solution

The solid Zn target was taken from Fluka company ,(united-states, product in 2015). with high purity 99.999%. The sheet of Zinc cut into small piece with dimensions of (2×2) cm^2 after that immersion the target in the solution used.

3.4 Laser Ablation System

Figure (3.3) shows the experimental setup for synthesis of ZnO nanoparticles. Glass container was applied as a cell, and the Zn target placed on the bottom of this container filled with 3 ml of distilled water or other solution. The cell holder rotates of 9 rpm to provide uniform ablation and to avoid formation of a deep ablation trace due to repeated laser pulses on same spot to help mix the solution as well. The laser ablation process, which includes Nd:YAG laser of wavelength 1064 nm or 532 nm, type of solvent, type of substrate and laser energy used. The ablation process is done at room temperature. The target (Zn) (purity of 99.99%) has been immersed in water or aqueous solution, and fixed at bottom of glass vessel container. The parameters, which effect on the quality of thin films prepared in this method stated briefly, as following:

Figure (3.3): Experimental setup for nanoparticles synthesis by PLA process [82].

3.4.1 Laser Ablation Source

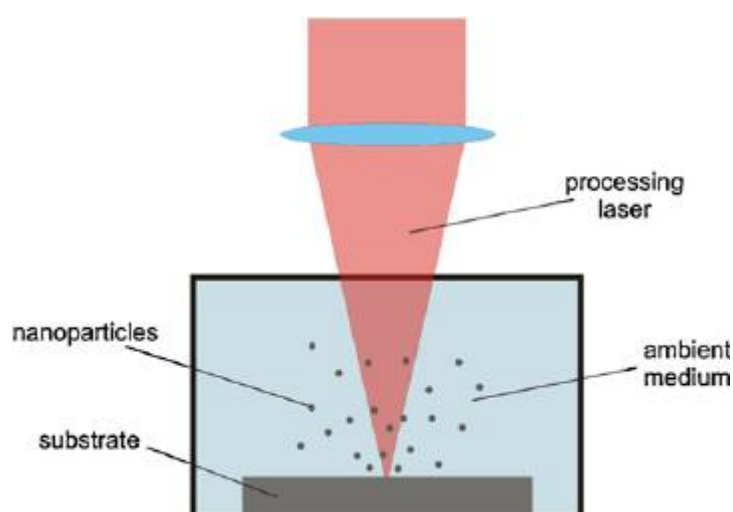Nd:YAG laser system type Huafei providing pulses at 1064 nm wavelength who was used as source for ablation of Zn target. Different laser energies per pulses of (600,700 and 800) mJ, pulse duration is 10

ns, repetition rate of 1Hz, effective beam diameter of 4.8 mm and the number of laser pulse of 1000, 1500 and 2000 pulses have been used in this work.

3.4.2 Solution Types

In present work, distilled water (DW), and methanol have been used as a solvents.

3.4.2.1 Distilled Water

Distilled water (DW) represents a base medium for all samples and solution to produce nanoparticles in this work. Even such water is entirely pure; however, it is contaminated by salts ions, dissolved gases and dissolved materials. Distilled water was prepared in our laboratory in glasses containers to avoid the contamination

3.4.2.2 Methanol Solution

Absolute methanol (with purity 96%) was used as ablation medium in this study. Compared to other solvents, methanol provides a relatively inert environment for the production of nanoparticles. In addition, it has special property to exclude the oxide layer and to prevent the nanoparticles from oxidation.

3.5 Preparation ZnO thin film using Sol gel technique

In regard with spin coating method, the solution prepared by mixed of zinc acetate as solvent and monoethanol amine MEA as stabilizer of ratio 4:1 dissolved in 50 ml ethanol. To make sure that the solution is homogeneous, the solution treatments using magnetic stirrer and hot plate at temperature of 80°C for 1hour.

3.6 The Characterization Instruments

The structural properties using XRD, Scanning electron microscopy (SEM), Energy dispersive X-ray (EDX) have been characterized. In addition, the optical properties using UV-Visible spectrometer have been studied, as following:-

3.6.1 Instrument used for Structural Properties Analysis

3.6.1.1 XRD Measurement

In order to explain the structural properties, the nature and the crystal growth of the deposited films, X-ray diffraction measurement had been done according to either the ASTM (American Standard of Testing Materials) or JCPD cards no. 36-1451 using Philips PW 1050 X-ray diffract meter of 1.54 $A^°$ from Cu- kα. By using XRD result the crystalline size (D) and FWHM could estimate and calculated using eq (2.38).

3.6.1.2 Scanning Electron Microscope (SEM)

In this study the (SEM) a scanning electron microscopy (INSPECT S50) equipped with energy dispersive X-ray. According to the microscope specifications, resolution up to 7.0 nm at 3 KV (in high vacuum mode) ensured, while magnification reported to be in the range of 13-1000000X; though, these data is dependent on the characteristic of each sample. It can be different depending on the sample components like samples with heavier elements lead to obtaining analysis that is much more accurate.

3.6.1.3 Energy Dispersive X-ray (EDX)

In this study, the EDX analysis software was sourced from Oxford Instruments Analytical Ltd. and was used to identify the elements in the samples. All measurements were performed at an accelerated voltage of 10 kV. The electron beam current was controlled by adjusting the spot size of the beam using the SEM control.

3.6.2 Instrument Used for Optical Properties Analysis

A double –beam UV-IR 210A Spectrophotometer is used to measure the transmittance and absorption of ZnO film deposited at different conditions within the wavelength range (300-900 nm) by using the data given from this instrument, the absorption coefficients and transmission have been calculated [83].

3.7 Thickness Measurement

In these work measured the film thickness which using SEM method; this method was used to get the sample which was broken and coated with gold for nonoconductive substrate. SEM micrographs of the cross section of thin films at a tilt angle of 80 degrees where the sample was mounted with the film on top.

Chapter Four

Result and Discussion

4.1 Introduction

In present chapter, firstly, the antireflection film with zero reflectance condition have been design and the optical performance of glass substrate examined using UV-V spectroscopy. Then, the structural and optical properties of ZnO nanoparticles deposits on glass and Psi substrates using PLA and Sol-Gel techniques have been discussed. The effect of laser pulses number of 1000, 1500, and 2000 pulse at energies of 600, 700 and 800 mJ with methanol and distilled water solvent have also been studied. Over the results, the work divided into two main parts: design of single antireflection coating layer and structural and optical properties of the prepared films, which could divided into three sub-parts too: preparation techniques (PLA and sol-gel), laser ablation conditions (number of pulses, energy, and solvent type), and substrates type (glass and PSi) as following:-

4.2 Single layer

Antireflection coating system (SL-ARC$_S$) used to obtain zero reflection condition of signal layer design, the modified characteristic matrix have been employed (see section **2.4)** . For this purpose, the design wavelength (λ_d) was selected to be 1064 nm and the incident beam consider to be normal, then the theoretical reflection values of uncoated and coated with ZnO film on (glass and silicon substrates) are calculated depend on the following equation [84] :

$$R = (\frac{n_0-n_s}{n_0+n_s})^2 \qquad \textbf{For uncoated substrate} \qquad (4.1)$$

and

$$R = \left(\frac{n_0 n_s-n_1{}^2}{n_0 n_s+n_1{}^2}\right)^2 \qquad \textbf{For coated substrate with film} \qquad (4.2)$$

Where R: represent to the reflection, n_o: the air refractive index , n_s: substrate refractive index and n_1: film refractive index

The reflection values of both cases are formulated in Table 4.1 as shown below where, the refractive index of glass and silicon are 1.52 and 3.4 at wavelength of 550 nm.

Table (4-1):

Theoretical reflection results of uncoated and coated with ZnO film substrates

Structure	Reflection	Remark notice
Glass substrate	4%	Satisfied zero reflection of glass eq (4.1) without coated
Si substrate	30%	Satisfied zero reflection of glass eq (4.1) without coated
ZnO/glass substrate	20%	Satisfied zero reflection of glass eq (4.2) for coated
ZnO/Si substrate	0.6%	Satisfied zero reflection of glass eq (4.2) for coated

Note that ZnO deposited on PSi substrate gives better results than glass substrates due to convergence of refractive index between ZnO and silicon.

In this work, ZnO thin film used as antireflection layer (ARC_s) with optical path (nd) equal to quarter wavelength (λ/4) or multiply it. Thus, the thickness measured to be 100 nm for film deposited on glass and PSi substrates depend on [85]:

$$nd = \lambda/4 \quad \text{So, d=}\lambda\text{/4n} \tag{4.3}$$

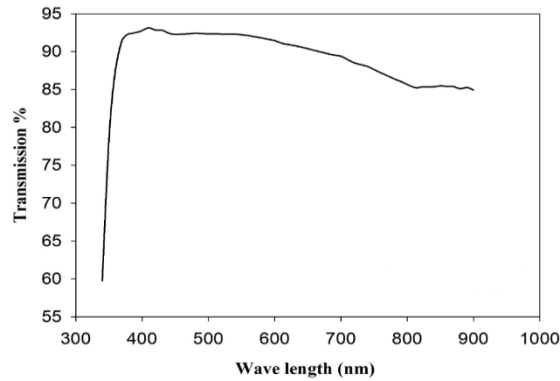The transmittance curve as function of wavelength shown in Figure (4.1)

Figure (4.1): Transmission curve as a function of wavelength of ZnO thin film on glass substrate.

4.3 Structural Results of ZnO ARC$_S$

The effect of fabrication conditions such as laser system parameters including the influence of laser pulses number, energy, solvent type, and substrate type on the structural properties of ZnO nanoparticles prepared using PLA and sol-gel techniques have been studied. These effects characterized using XRD analysis to study the structure nature of prepared films and corresponding properties such as, prefer diffraction peak, lattice parameters, FWHM, crystalline size, strain and dislocation density. As well as, the morphology of the surface of prepared films have been characterized using SEM, and EDX spectroscopies.

4.3.1 X-Ray Diffraction (XRD) Results of ZnO Nanoparticle by PLA Technique

Firstly, the PLA technique used to prepare ZnO nanoparticle and related parameters will study as following:

4.3.1.1 The effect of laser pulses number

Figure (4.2) show the XRD pattern of ZnO nanoparticle on glass substrate with laser pulses number of 1000, 1500, and 2000 pulse at energy of 700 mJ in methanol and distilled water. This Figure revealed that the ZnO films have hexagonal polycrystalline structure nature with lattice parameter of samples dissolve in methanol c=5.130, 5.128 and 5.200, respectively and of samples dissolve in distilled water c= 5.179, 5.262 and 5.217, respectively. Figure (4.2.a) show that the diffraction peaks of ZnO nanoparticle in methanol on glass substrate were at 34.42°, 36.25° and 47.53°, which corresponding to the orientations of (0 0 2), (101) and (1 0 2) . Figure (4.2.b) show that the diffraction peaks of ZnO nanoparticle in distilied water on glass substrate were at 34.42°, 36.25°, 47.35°, 56.60° and 66.37°, which corresponding to the orientations of (0 0 2), (1 0 1), (1 0 2), (1 1 0), and (1 1 2). The discussion of XRD results will depend on the prefer orientation (0 0 2) ZnO. The increasing in the intensity of the peaks of sample prepared in PLA method on 1000,1500 and 2000 pulses by methanol and distilled water solution attributed to the increasing in crystal structure (crystility) of decreasing of the defect with in the structure. The position miller indices, lattice constant, FWHM, crystalline size and dislocation density of the above condition have been summarized in Table (4.2)

-a-
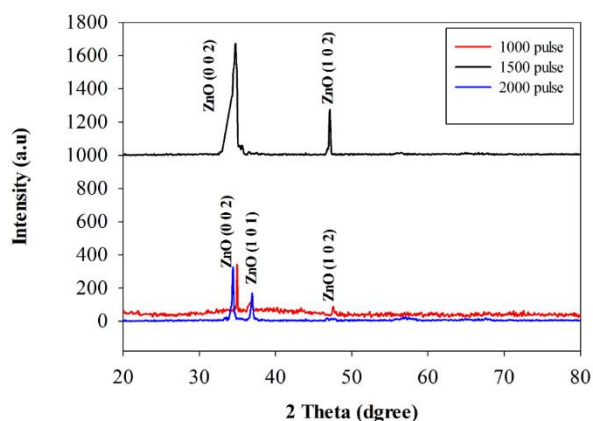
-b-

Figure (4.2): The XRD pattern of ZnO nanoparticle on glass substrate with laser pulses number of 1000, 1500, and 2000 pulse at energy 700 mJ **a-** methanol solvent **b-** distilled water solvent.

4.3.1.2 The effect of laser energy

Figure (4.3) shows the XRD pattern of ZnO nanoparticle on glass substrate with laser pulse number of 1500 pulse for energies of 600, 700 and 800 mJ dissolved in methanol. This Figure revealed that the ZnO films have hexagonal polycrystalline structure nature with lattice parameter c=5.230A°, 5.128° and 5.137A° respectively. The diffraction peaks were at 34.90° and 36.17 A°, which corresponding to the orientations of (0 0 2), and (1 0 1). it is clear that there is no change in phase and the optimal energy was at 700 mJ.
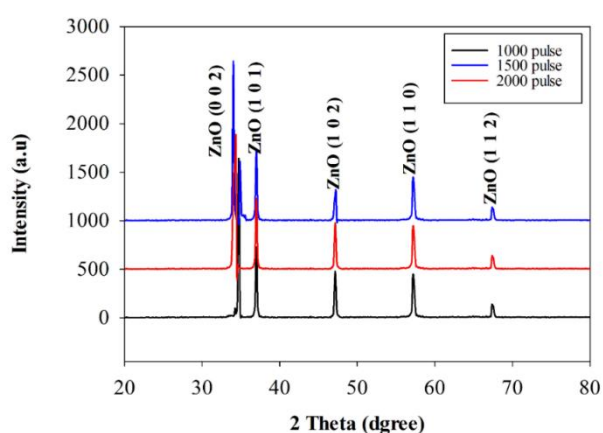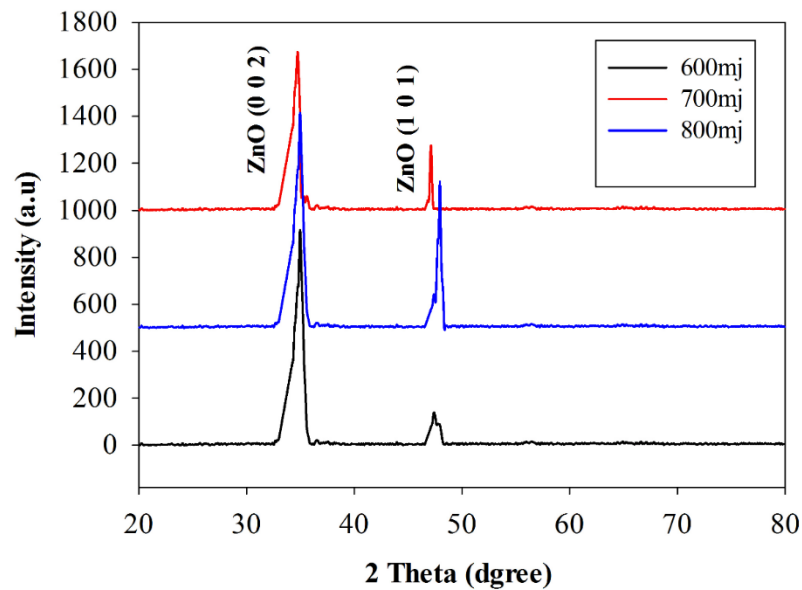
Figure (4.3): The XRD pattern of ZnO nanoparticle on glass substrate with laser
pulses number   of 1500 pulse at energy 600 mJ ,700 mJ and 800mJ .

4.3.1.3 The Effect of solution Type

Figure (4.4) show the XRD pattern of ZnO nanoparticle on glass substrate with laser pulse number of 1500 pulse at energy 700 mJ in distilled water and methanol solutions. Figure (4.4) revealed that the ZnO films have hexagonal polycrystalline structure in nature with lattice parameter c=5.262 A $^\circ$ and 5.217 A $^\circ$, respectively. In distilled water solution were at 34.95 $^\circ$, 36.52 $^\circ$, 47.53 $^\circ$, 56.60 $^\circ$ and 66.37 $^\circ$, which corresponding to the orientations of (0 0 2), (1 0 1), (1 0 2), (1 1 0) and (2 0 0) and in methanol solution were at 34.95° and 47.53° corresponding to the orientations of (0 0 2) and (1 0 2). it is clear that there is no change in phase. They appear of all peaks regarding the polycrystalline ZnO sample prepared in PLA method on 1500 pulses by distilled water solution at energy of 700 mJ means the sample became more homogeneous and the defect is less as pussible.
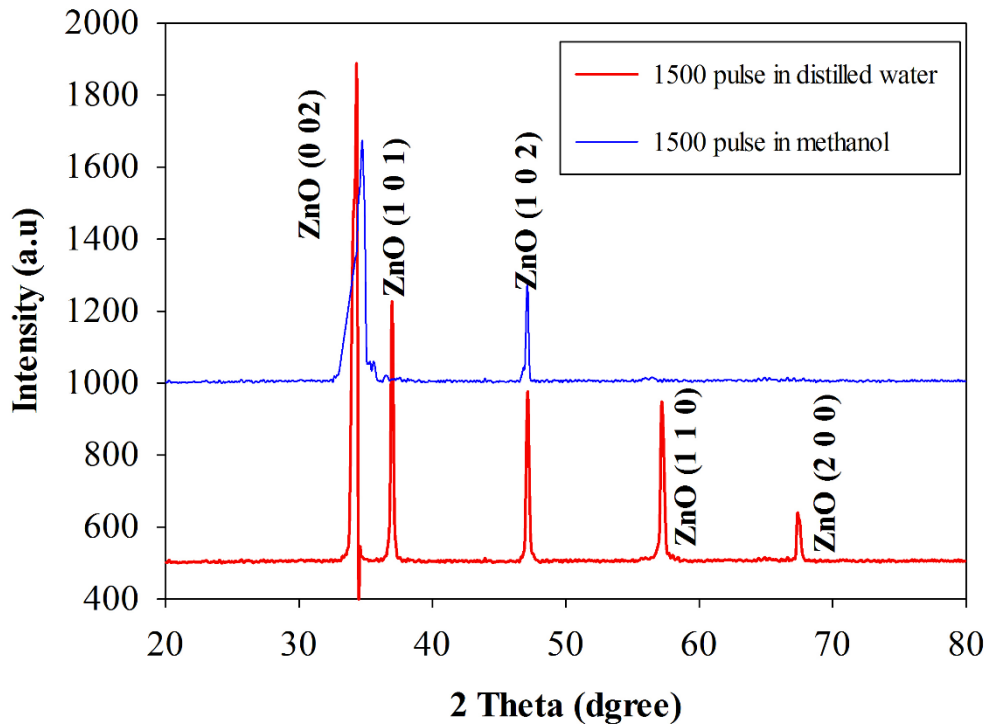
Figure (4.4): The XRD pattern of ZnO nanoparticle on glass substrate with laser pulses number of 1500 pulse at energy 700 mJ in distilled water and methanol solvents.

4.3.1.4 The effect of substrate type

Figure (4.5) show the XRD pattern of ZnO nanoparticle on glass and PSi substrates respectively, with laser pulses number of 1500, pulse at energy 700 mJ in distilled water solution. Figure (4.5) revealed that the ZnO films have hexagonal with lattice parameter c=5.128 A $^\circ$ and 5.217 A$^\circ$ for a sample prepared on glass and PSi substrates respectively. This Figure show that the diffraction peaks of ZnO nanoparticle on glass substrate were at 34.95 $^\circ$, 36.25 $^\circ$, 47.53 $^\circ$, 56.60 $^\circ$ and 66.37 $^\circ$, which corresponding to the orientations of (0 0 2), (1 0 1), (1 0 2) , (1 1 0), and (2 0 0). And on PSi substrate were at 34.95 $^\circ$ and 56.60 $^\circ$ which corresponding to the orientations of (0 0 2) and (1 1 0). These results is agreement with those given in JCPD data card no. 36-1451 and it is clear that there is no change in phase for all peaks expected for (1 1 0) which may be because the effect of created a heating treatment depending on substrate type.
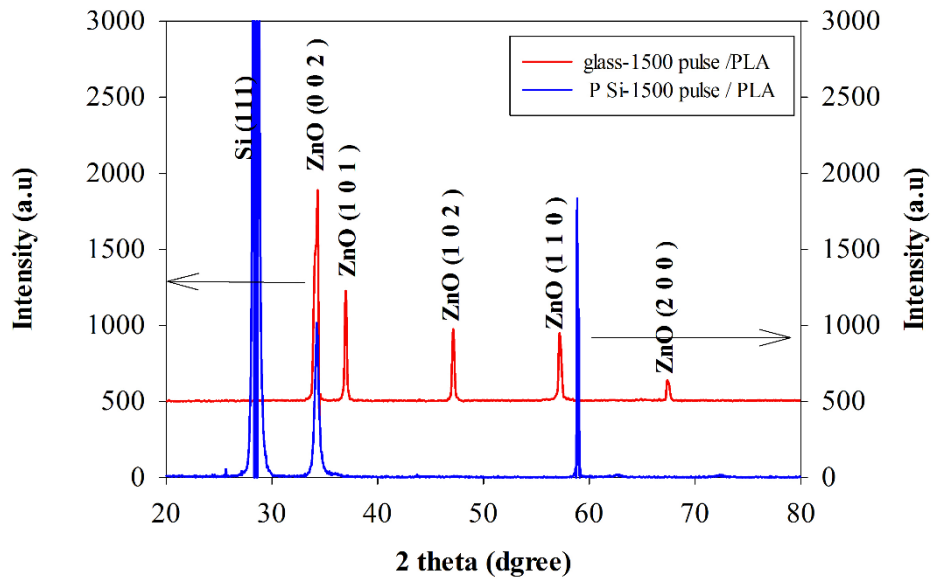
Figure (4.5): The XRD pattern of ZnO nanoparticle on glass and Si substrates prepared using PLA method with laser pulses number of 1500 pulse at energy 700 mJ dissolved in distilled water solution.

4.3.2 X-Ray Diffraction (XRD) Results of ZnO Nanopartical by Sol-Gel Technique

Secondly, the Sol-Gel method used to prepare ZnO nanoparticle on glass and PSi substrates with concentration ratio of zinc acetate to monoethanolamain (MEA) was 1:4, 3000 rotation per minutes for 30 second have been compared with that prepared using PLA technique. Figure (4.6a) revealed that the ZnO films have hexagonal polycrystalline structure in nature with lattice parameter c=5.199 and 5.206 for sample prepared on glass and PSi substrates respectively. In addition the XRD peaks of 34.475◦, 36.17◦, 47.57◦, and 56.17◦ which correspond to orientation (0 0 2), (1 0 1), (1 0 2), and (2 0 0) respectively of ZnO thin film on glass substrate. Theses peaks confirmed that the films are polycrystalline in nature .Figure (4.6b) show the XRD peak of 34.425◦, 36.17◦, 47.57◦, and 66.73◦ which correspond to orientation (0 0 2), (1 0 1), (1 0 2), and (2 0 0) respectively of ZnO thin film on PSi substrate. These results revealed that the phase between the glass and PSi

substrates has no changed. All these result in regarding the previous sub section are summarized in Table (4-1).
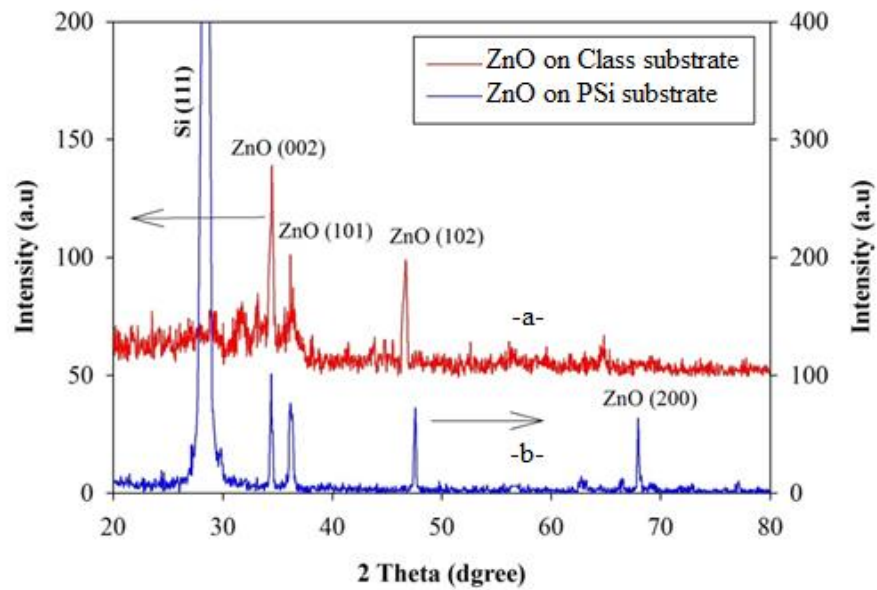

Figure (4.6): The XRD pattern of ZnO nanoparticle a- on glass and b- on PSi substrates prepared using sol gel method.

Table (4-2): The obtained result of the XDR for ZnO nanoparticles at different (pulse, energy, solvent, method).

In summary and depend on the results especially on table (4.1), it is possible to conclude that the best method to preaper ZnO was PLA method with the optimal condition of preparation parameters were laser energy of 700 MJ, laser pulses of 1500 pulse and methanol solution. In addition, the using of P-Si as substrate was the best a recommended with glass substrate.

4.4 Scanning Electron Microscopes (SEM) Results

Figure (4.7) show SEM images of ZnO nanoparticle prepared using PLA with pulse laser ablation, at fixed energy of 700 mj and different pulses of 1000, 1500 and 2000 dissolved in methanol solution and deposition on glass substrate. It clear that the structure became as island and then cracking observed with increases the pulse number which attributed to interact of laser pulses with surface and may be reformed it by reconstructed the atom on the surface. The partials size was in nanoscale and it is seem like (cluster) at pulse number of 1500 which confirmed the XRD results.
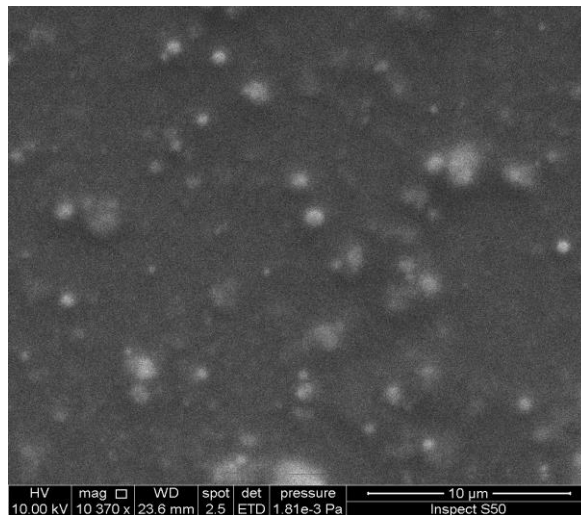
-a-
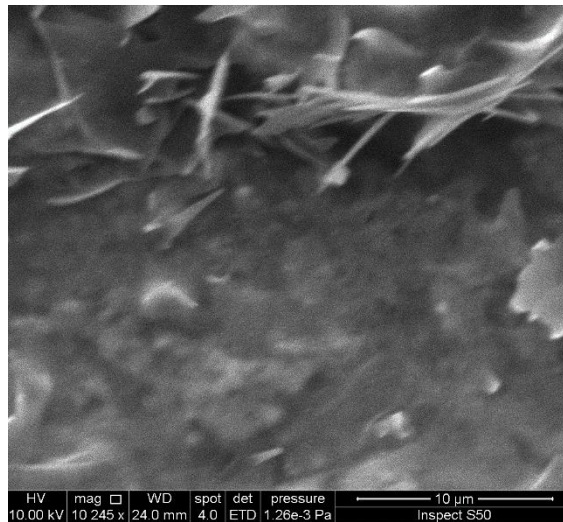
-b-
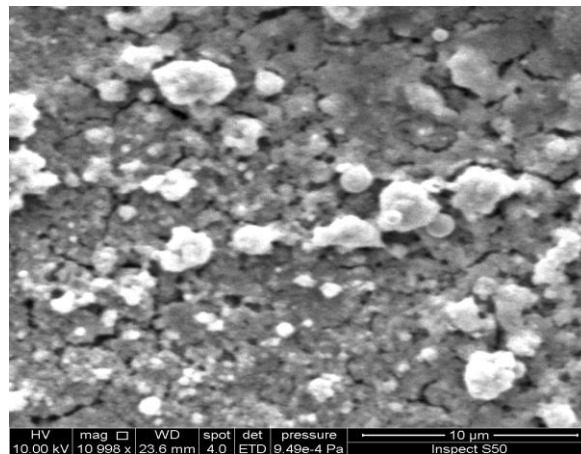
-c-

Figure (4.7): SEM images of ZnO thin film on glass substrate   prepared using PLA method in methanol solvent with energy 700 mj and pulses of a- 1000, b-1500, and c-2000 pulses with scaling bar of 10 μm

4.4.1 Thickness Measurement

The thickness of the ZnO film prepared of 1500 pulse with 700 mJ, has been measured using cross section of SEM image as shown in Figure (4.8) the average of thickness of film was 563 nm for all samples used. These result is agreement with the theoretical calculation in regared with design of single layer and with the weight method.
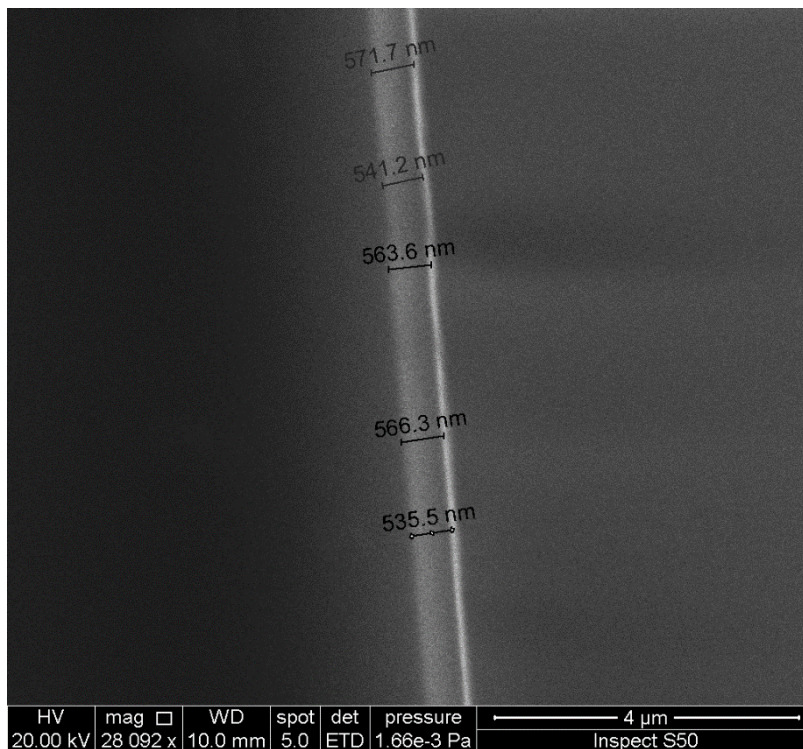
Figure (4.8): SEM cross section of ZnO thin film.

Figure (4.9) shows the EDX analysis which confirmed that the Zn and O elements are including in the prepared films on glass substrate using PLA method with energy of 700 mJ and at a- 1000 , b- 1500 , c- 2000 pulses in methanol solution.

Elements	Wt %
Zn	74
O	9
Au	17

Elements	Wt %
Zn	76
O	10
Au	14

Elements	Wt %
Zn	40
O	31
Au	29

Figure (4.9): EDX analysis of ZnO thin films prepared by PLA method on glass substrate with energy 700 mj at pulses a-1000, b-1500 and c-2000 pulses in methanol solvent

Figure (4.10) show SEM images of ZnO nanoparticle prepared using PLA with pulse laser ablation, at fixed energy of 700 mJ and different Pulses of 1000, 1500 and 2000 dissolved in distilled water solution on glass substrate. It clear that the surface become spongy at

1500 surface and then the roughness increased at 2000 pulse. The partials size was in nanoscale this result is agreement with XRD results.

-a-

-b-
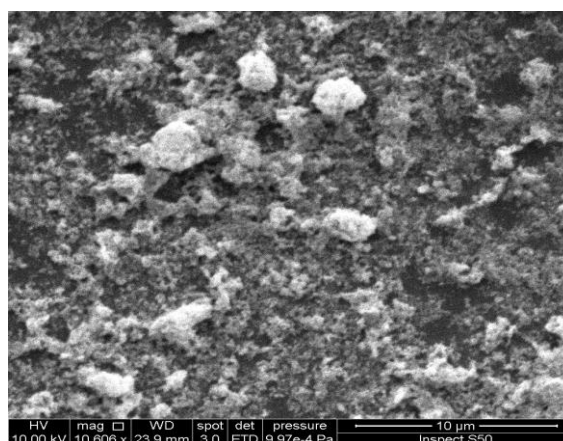
-c-

Figure (4.10): SEM images of ZnO thin film on glass substrate   prepared using PLA in distilled water solvent with energy of 700 mJ and pulse of a-1000, b-1500, and c-2000

Figure (4.11) show the EDX analysis which confirmed that the Zn and O elements is including in the prepared films on glass substrate

using PLA method with energy 700 mj and pulse number of at 1000,1500 , and 2000 pulses in distilled water solvent.

Elements	Wt %
Zn	75
O	15
Au	10

Elements	Wt %
Zn	72
O	9
Au	19

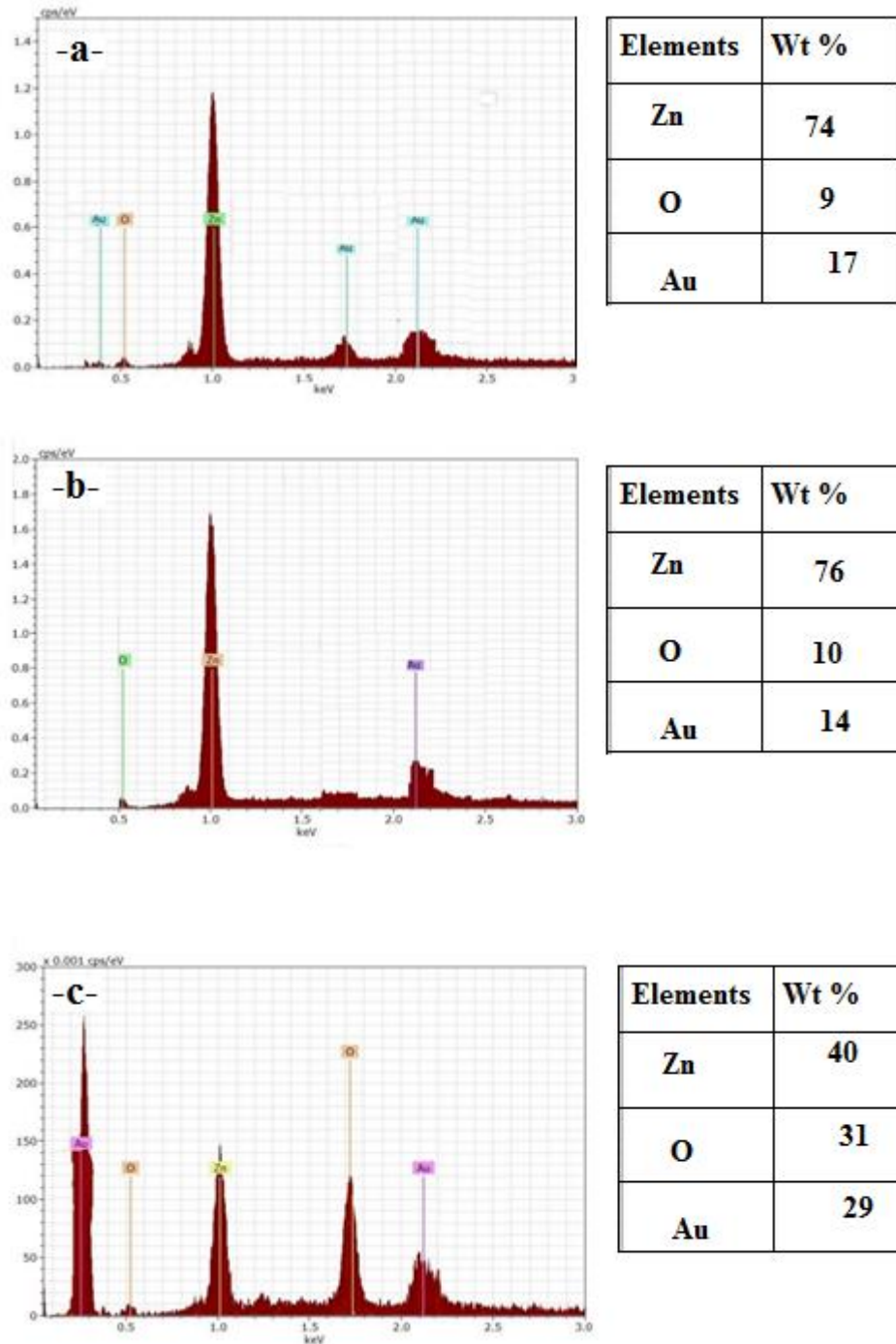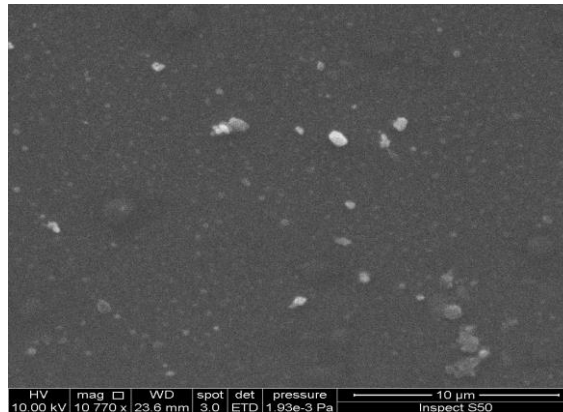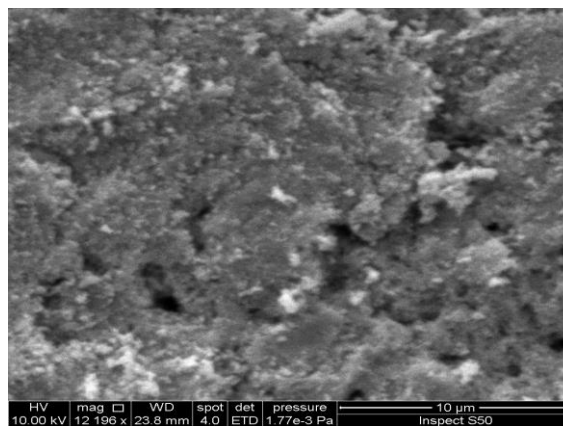| Elements	Wt %
Zn	71
O	14
Au	15
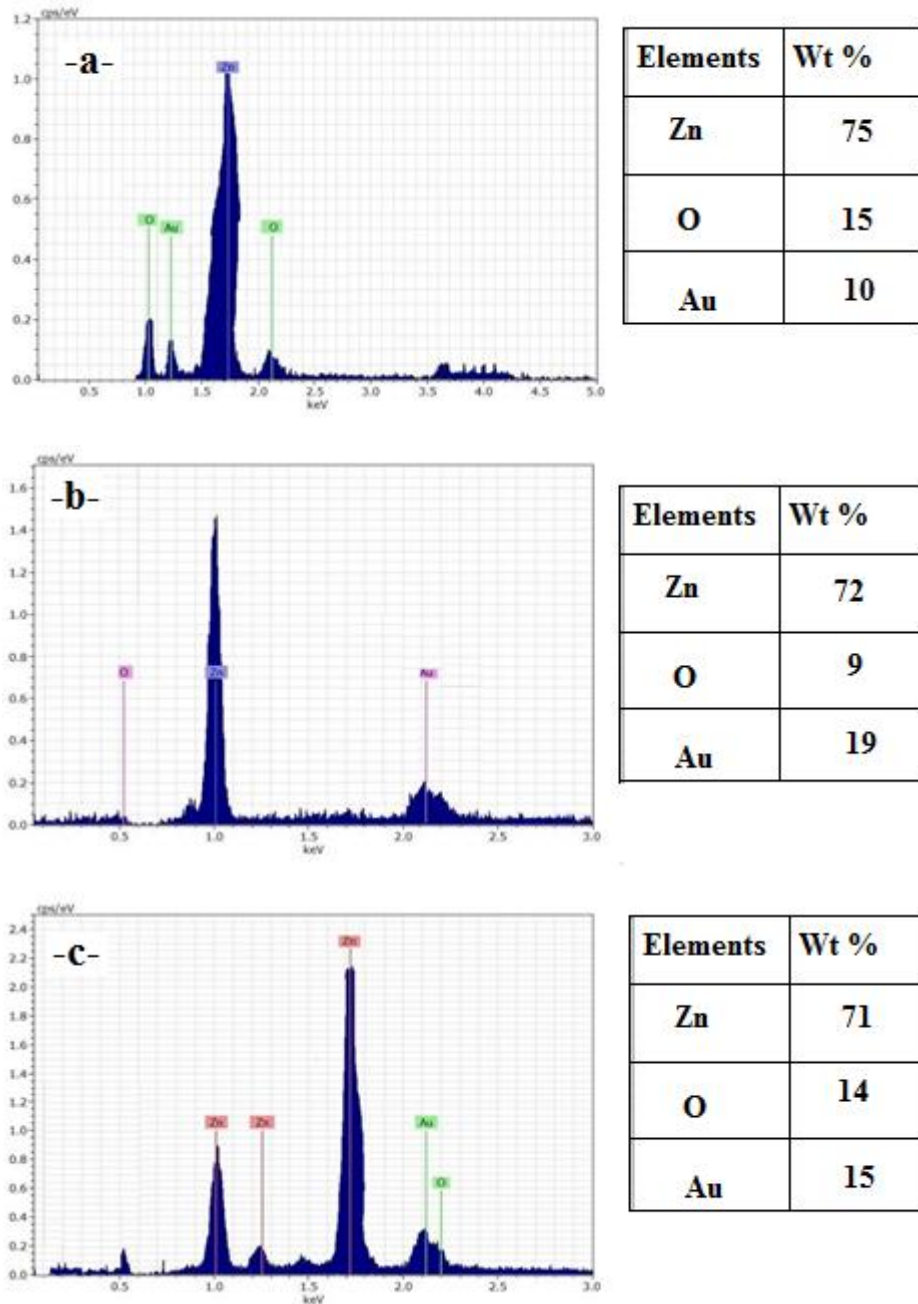
Figure (4.11): EDX analysis of ZnO thin films prepared by PLA method on glass substrate with energy of 700 mj and at pulse number a-1000, b-1500, and c-2000 pulses in distill water solvent.

Figure (4.12) show SEM images of ZnO nanoparticle prepared on glass substrate using PLA with energy of 600, 700 and 800 mJ at pulse number of 1500 pulse, dissolved in methanol solution. It clear that the

partials size is formed in nanoscale especially at energy 700 mJ which seem like (flower) structure We have more uniform nanoparticles in this case [31], while, at 600 mJ the surface look with various crystalline size and at 800 mJ the surface became more sponge with pore size in range of 100-1000 nm.This result is agreement with XRD results and open the door for more studies on this behavior.

-a-

-b-
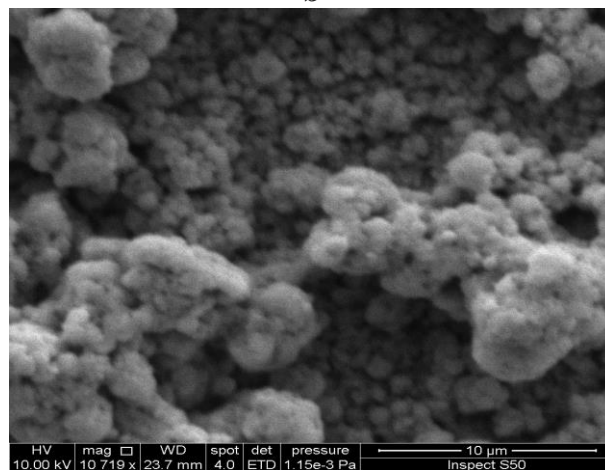
-c-

Figure (4.12): SEM images of ZnO thin film on glass substrate prepared using PLA at pulse number of 1500 and with energy of a-600, b-700 and c-800 mJ in methanol solution.

Figure (4.13) show the EDX analysis which confirmed that the Zn and O elements is including in the prepared films on glass substrate using PLA method with energy of 700 mJ and at a- 1000, b- 1500 and c- 2000 pulses in methanol solution.

Elements	Wt %
Zn	61
O	20
Au	19

| Elements	Wt %
Zn	53
O	13
Au	34

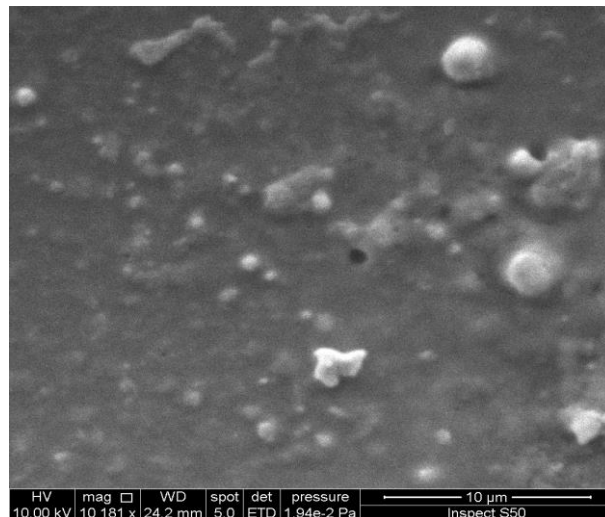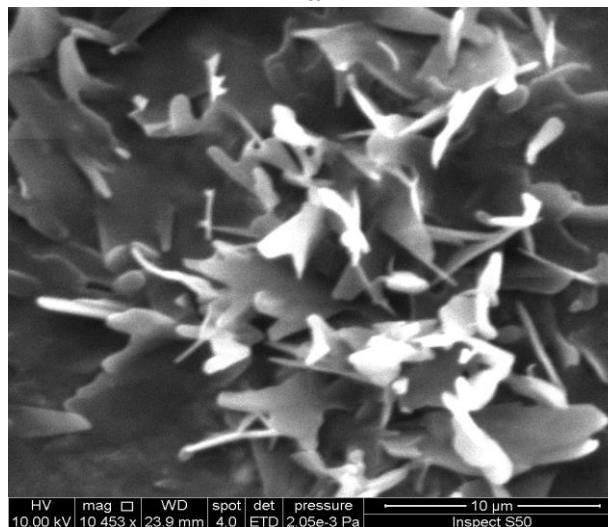| Elements	Wt %
Zn	80
O	8
Au	12
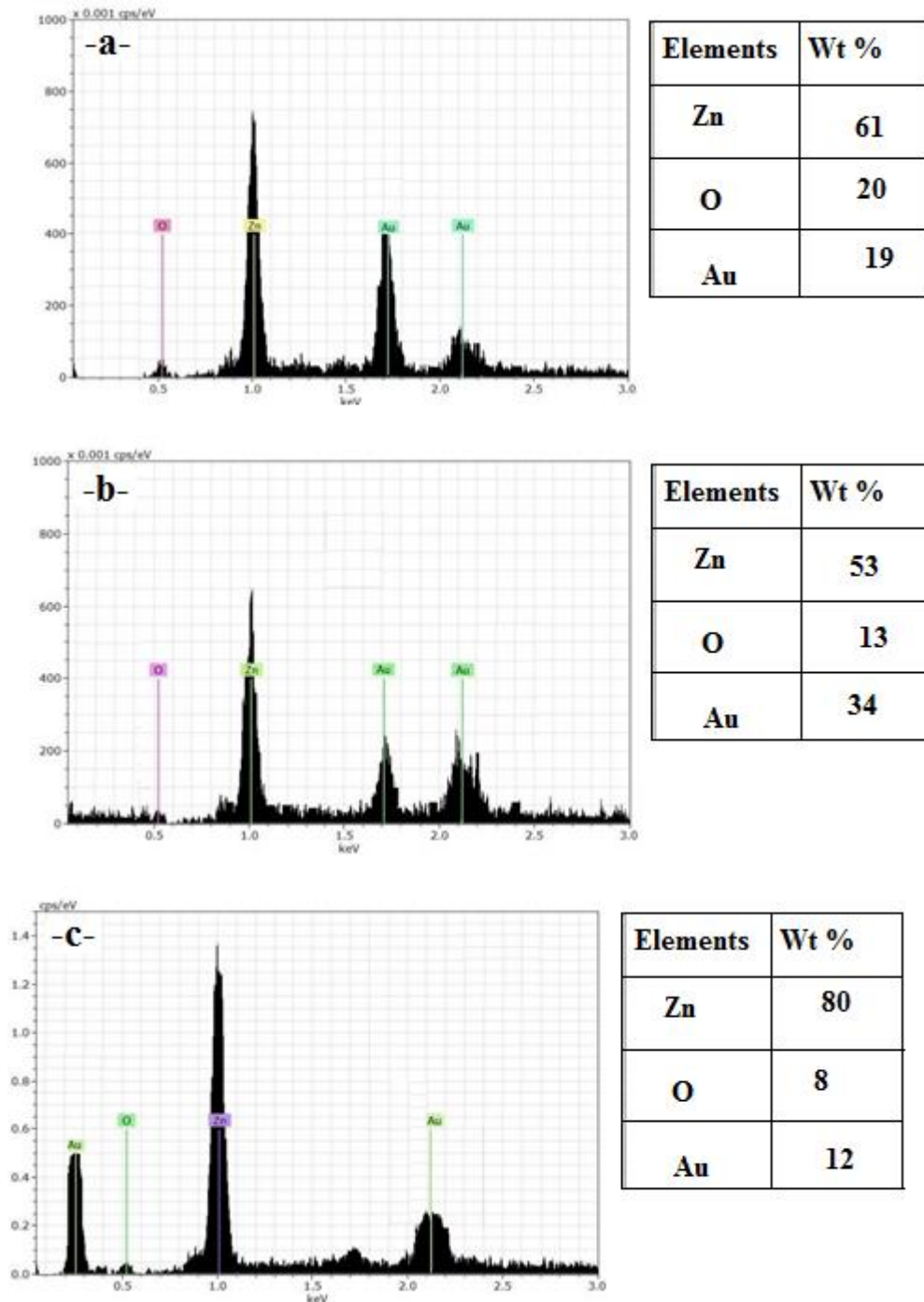
Figure (4.13): EDX analysis of ZnO thin films prepared by PLA method on glass substrate with energy of a-600 ,b-700, and c-800 mj in methanol solution.

Figure (4.14) show SEM images of ZnO thin film prepared using PLA with pulse laser ablation, with fixed energy of 700 mj and at Pulse 1500 dissolved in methanol solution, porous silicon substrate. It clear that the surface have pores with different size and different wall in surround and partials size was in nanoscale.this result is agreement with XRD results.
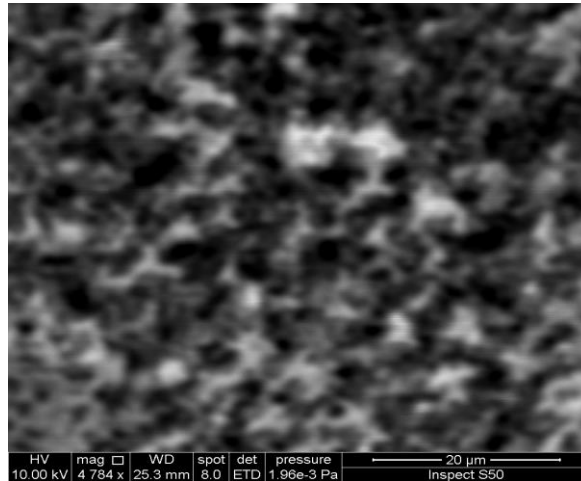
Figure (4.14): SEM images of ZnO thin film on Psi substrate prepared using PLA with pulse 1500 and energy 700 mJ in methanol solvent.

Figure (4.15) show the EDX analysis which confirmed that the Zn and O elements is including in the prepared films by PLA method on PSi substrate of methanol solvent.
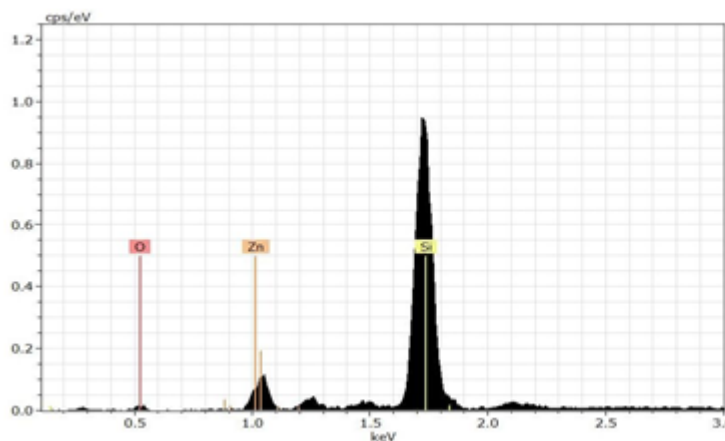
Elements	Wt %
Zn	85
O	5
Au	10

Figure (4.15): EDX analysis of ZnO thin films prepared by PLA method of P Si substrate in methanol solvent.

Figure (4.16) show SEM images of ZnO nanoparticle prepared using sol gel method. The surface morphology of fabricated ZnO thin films on silicon substrate have smooth with light and dark color   in compared with that film on glass substrate and sample on glass substrate have many folded which attributed to the high mismatching between the epilayer and substrate.
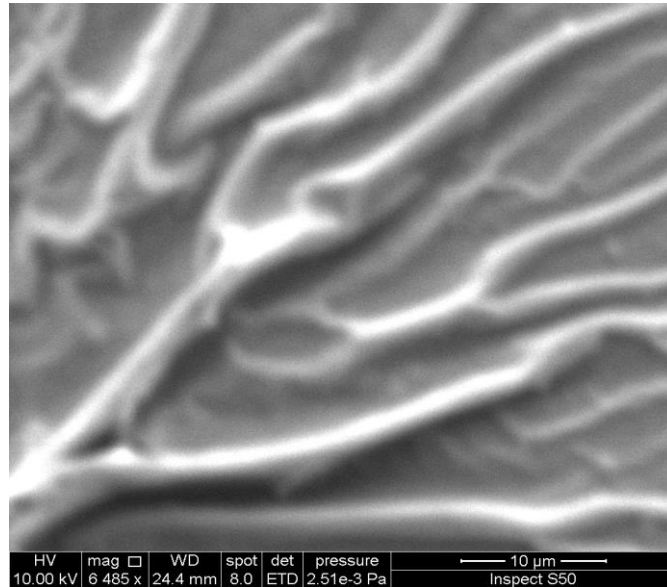
-a-
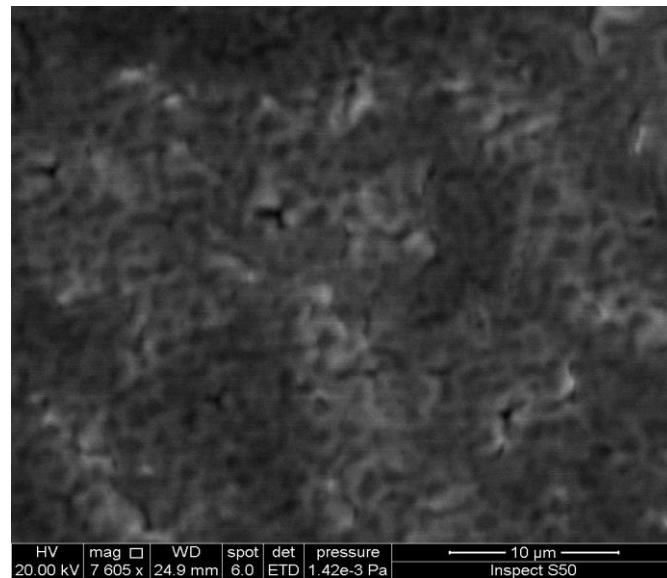
-b-

Figure (4.16): SEM images of ZnO thin film on a-glass substrate b-p si substrate prepared with sol-gel method with (3000) rotation through 10 minute.

Figure (4.17) show the EDX analysis which confirmed that the Zn and O elements is including in the prepared films on both glass and silicon substrate

Elements	Wt %
Zn	72
O	15
Au	13

Elements	Wt %
Si	54
Zn	22
O	10
Au	14
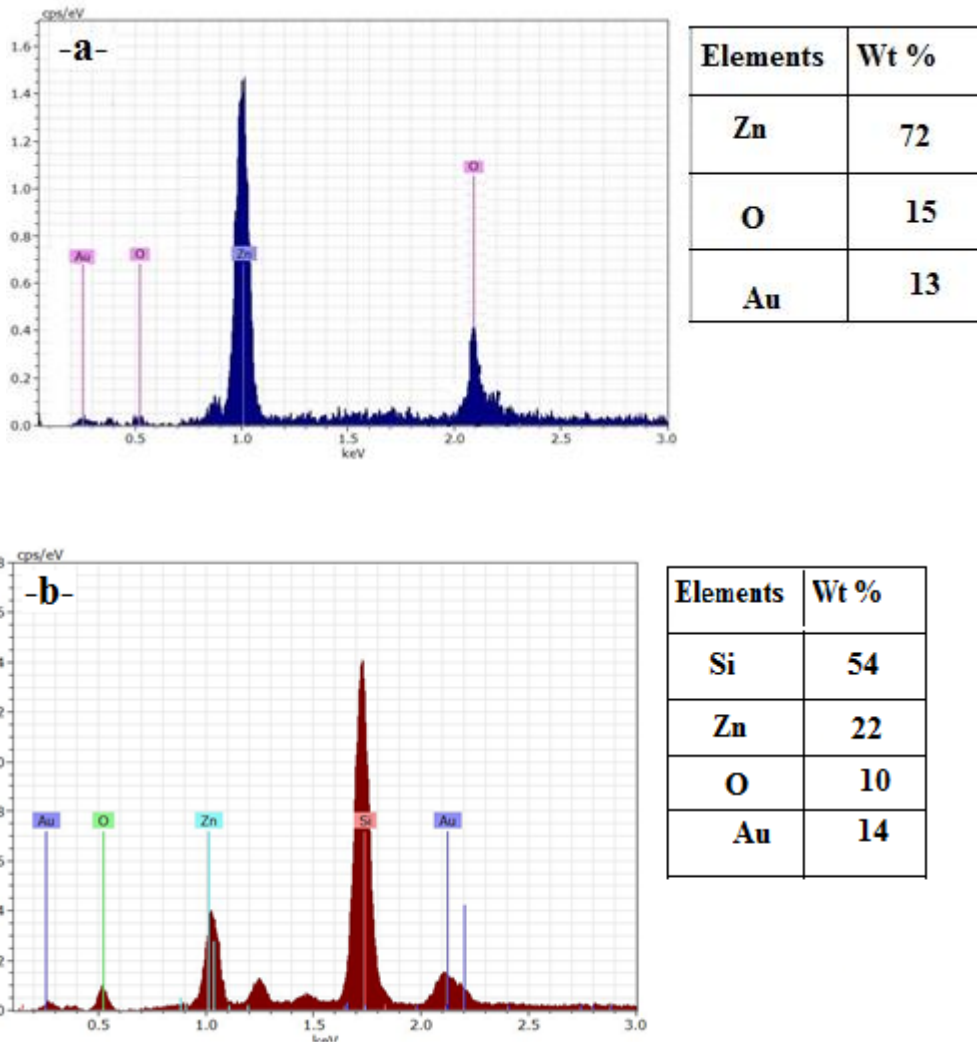
Figure (4.17): EDX image of ZnO thin films a-Glass substrate   b- pSi substrate
prepared using spin coating (sol gel) method

4.5 Optical Properties

The optical properties of the transparent conducting films depend mainly on the deposition techniques and the preparation conditions in this section the optical properties of ZnO thin films on glass substrate prepared using PLA and sol gel techniques have been discussed. by UV-Vis spectrophotometer are studied in the wavelength range from 200 nm

to 1100 nm, and study the effect of the laser pulses number, laser energy and solvent type on the optical properties of the prepared samples.

4.5.1 Effect of pulses number

The effect of the pulse number with 1000, 1500 and 2000 pulses of methanol and distilled water solutions on ZnO thin films is shown in Figure (4.18). It is found that the films have high transmission at long wavelengths reach to (90%) in the visible region. The optical transmission of ZnO thin films found to be decreases with increasing Pulses laser in methanol solution while the optical transmission of ZnO thin films found to be increasing with increases pulses laser in distilled water solution, which Attributed to satisfy the zero reflectance condition and the film became more transparent in regard with pulse.

Figure (4.18): Transmittance spectra as function of wavelength of ZnO thin films at different Pulses number of 1000, 1500 and 2000 dissolved in a- methanol solvent and b- distill water solvent .

High transmittance in distilled water solution indicates that the obtained films are of low impurities and have only few lattice defects [86]

Figure (4.19) show the effect of different laser pulse number with different type of solution. The different pulse in methanol solution It is found that the band gab energy increases with the increasing of laser

pulse number but in distilled water the energy band gap decrease with increased pulses.which mean that the blue shift of energy band gab is obtained . The energy band gap values depend in general on the film crystal structure, the arrangement and distribution of atoms in the crystal lattice also affected by crystal regularity. Attributed to the defect and high confinement effect since the structure going to be in nano scale in Table (4.3)
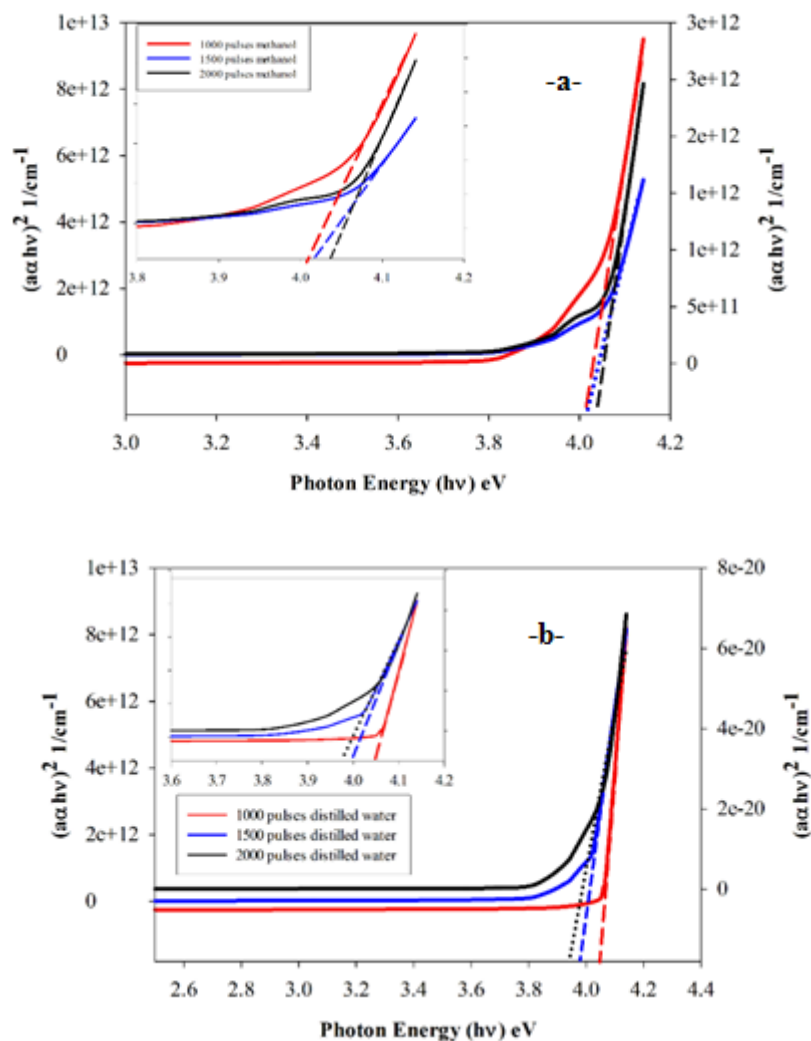
Figure (4.19): APlots of $(\alpha\, hv)^2$ verses photon energy (hv) of doped ZnO thin films at different of pulses number **a**- methanol solvent **b**- distilled water solvent.

Table (4.3):

Experimental result for different pulse laser number.

Pulse No. type of solvent		Eg (ev)
As-prepared in methanol solvent		3.37
1000 1500 2000	Methanol	4.01
		4.02
		4.03
As-prepared		3.37
1000 1500 2000	Distilled water	4.05
		3.97
		3.95

The band gap value increases as laser energy increasing, this could be linked to defects increase with decreasing in grain size because band gap value related to the crystalline of thin film [87].

4.5.2 Effect of Laser Beam Energy

The effect of the laser energy with 600,700, and 800 mJ on the optical properties of ZnO thin film prepared by PLA technique dissolved in methanol at pulses number of 1500 pulse is shown in Figure (4.20). It is found that the films have high transmission at wide range of long wavelengths (300-1100) reach to (90%) in the visible region. The optical transmission of ZnO thin films found to be decrease with increase laser energy, which Attributed to satisfy the zero reflectance condition and the film became more transparent in regard with pulse.

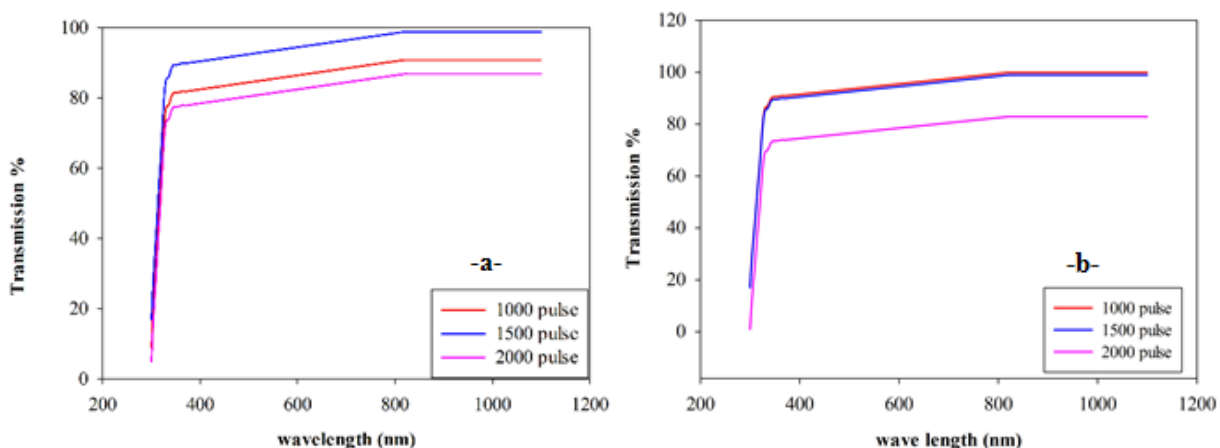Figure (4.20): Transmittance spectra of ZnO thin films at different laser energy with 600,700 and 800 mj of methanol solvent.

Figure (4.21) show the direct band gap values for ZnO thin film at different laser beam energy with 600, 700 and 800 mJ. The band gap value increases as laser energy decreasing, this could be linked to defects decrease with increasing in grain size because band gap value related to the crystalline of thin film also this due to formation of sub band between the band gap and conduction band [34]. as shown in Figure (4.21) and these results summarized in table (4-4).

Figure (4.21): APlots of $(\alpha h\nu)^2$ verses photon energy (hν) of doped ZnO thin films at different laser energy.

Table (4-4): Experimental result for different laser energy.

Laser beam energy (mJ)	Eg(ev)
As-prepared	3.37
600	4.06
700	4.02
800	4.01

4.5.3 Effect of Solution Type

Figure (4.22) show the effect of solvent type of ZnO on the optical performance. It clear that the films have high transmission at long wavelengths reach to (90%) in the visible region. The optical transmission of ZnO thin films found to be decreases in methanol solvent while increase in distilled water solvent, which attributed to satisfy the zero reflectance condition and the film became more transparent in regard with pulse.
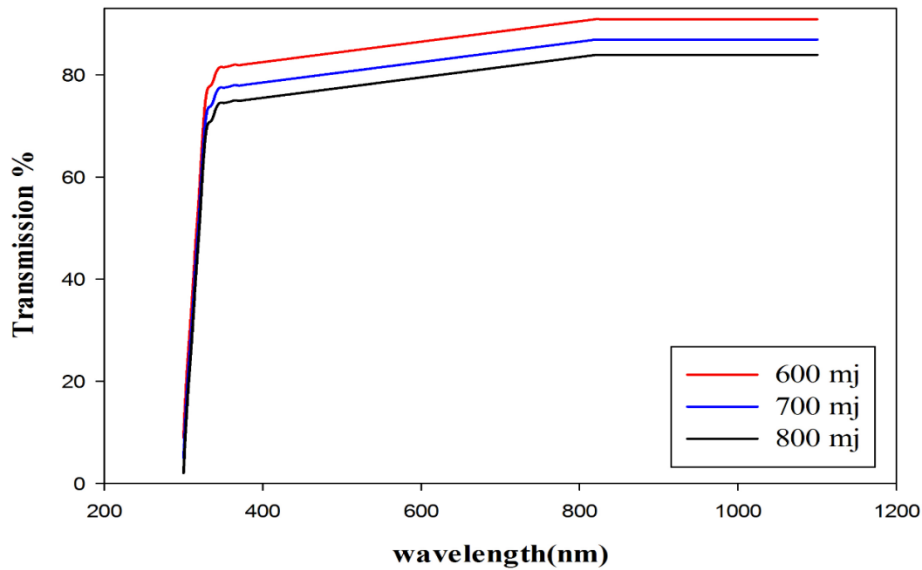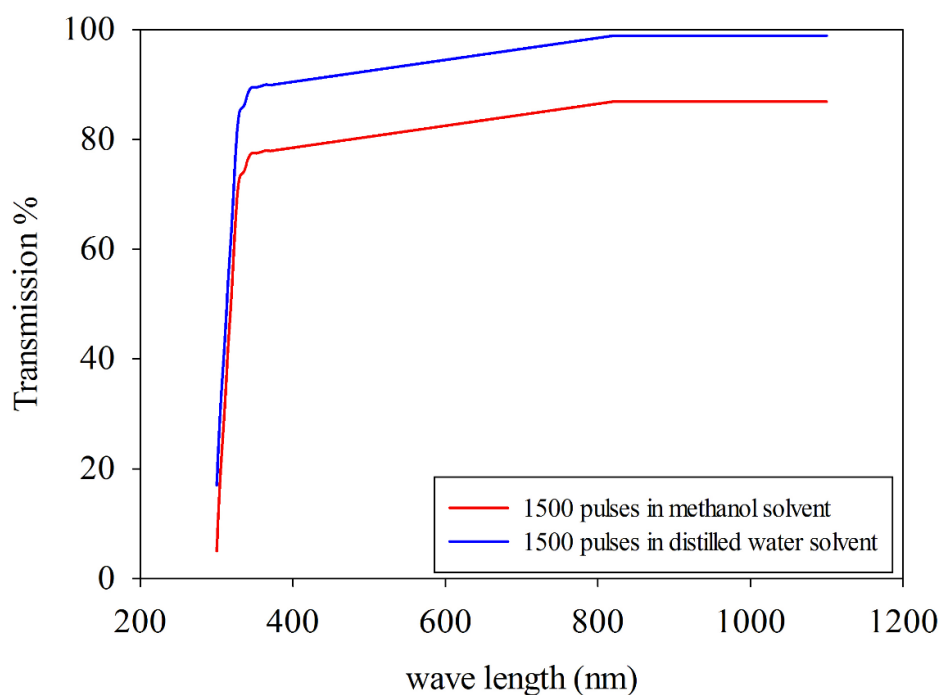

Figure (4.22): Transmittance spectra of ZnO thin films at different solvent type (methanol and distill water) solvent respectively.

The energy bang gap of methanol and distill water solvent as function of $(\alpha h v)^2$ has been examined. The results revealed that the value of energy band gap have blue shift toward the high energy band gap which attributed to the defect through the synthesis and may be high confinement effect occurred, since the structure became in nanoscale as mention in SEM results. These results show in Figure (4.23) and summarized in Table (4.5).
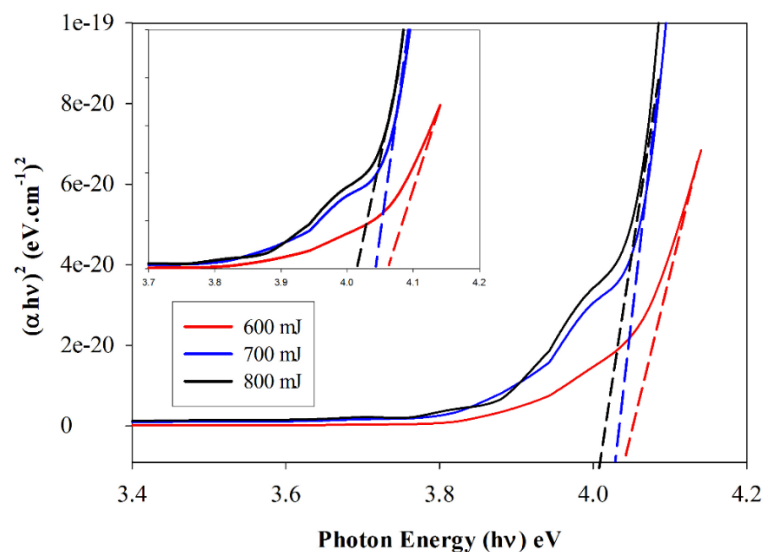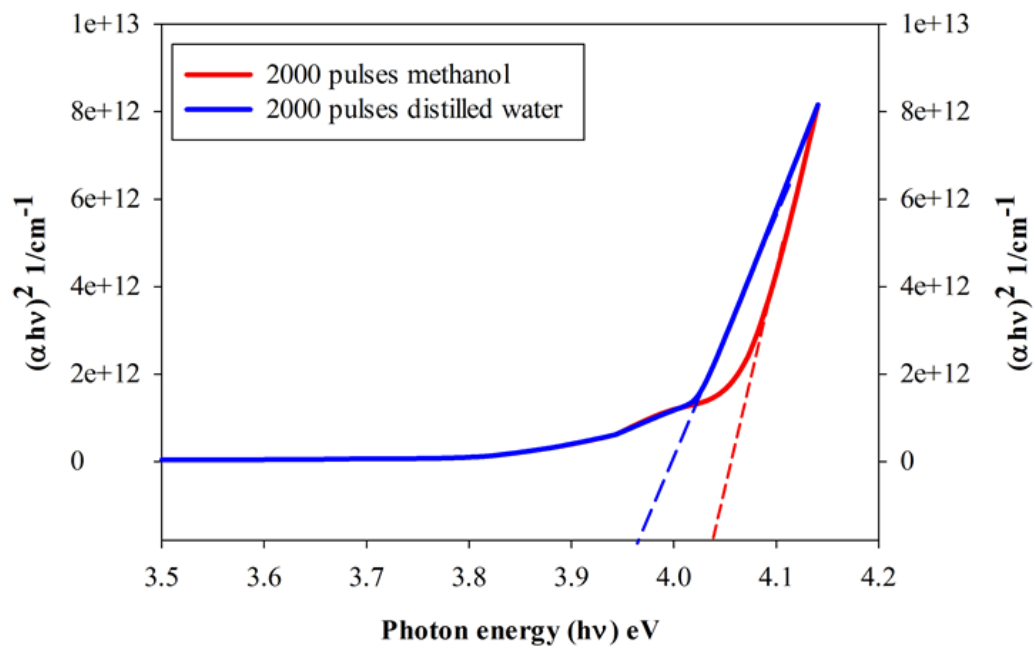

Figure (4.23): A plots of $(\alpha\ hv)^2$ verses photon energy (hv) of doped ZnO thin films of different solvent type.

Table (4-5):

Experimental result 2000 pulse of different solvent.

2000 pulse of solvent type	*Eg(ev)*
As-prepared	3.37
2000 pulse in methanol	4.03
2000 pulse in distill water	3.95

4.6 Optical Properties Results of ZnO Nanopartical by Sol-Gel Technique

In sol gel method the optical properties founded the substrate coated have high transmission at wide range of long wavelengths (300-1100) reach to (90%) in the visible region Compared with uncoated. attributed to satisfy the zero reflectance condition and the film became more transparent in regard   in comparison with uncoated substrate.as shown in Figure (4.24).
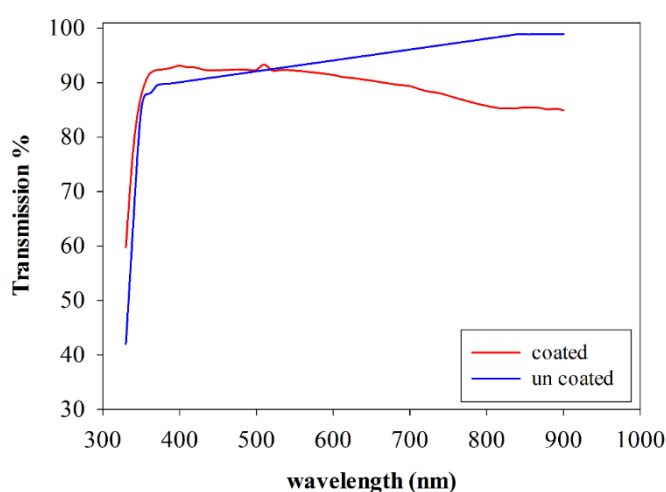
Figure (4.24): Transmittance spectra of ZnO thin films in case of coated and uncoated the substrate.

The energy bang gap of spin coating method as function of $(\alpha \, h\nu)^2$ has been examined. The results revealed that the value of energy band gap have blue shift toward the high energy band gap which attributed to the defect through the synthesis   and may be high confinement effect occurred, since the structure became in nanoscale as mention in SEM results. These results show in Figure (4.25)
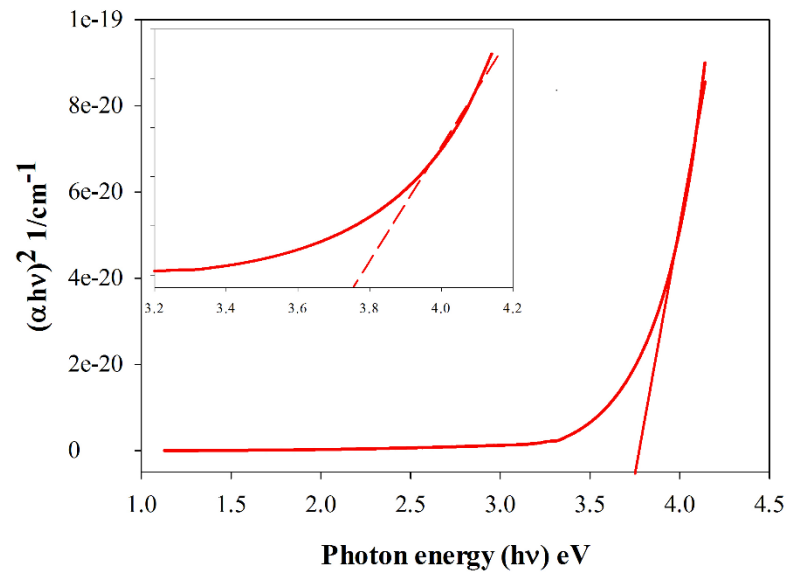
Figure (4.25): A plots of $(\alpha\, h\nu)^2$ verses photon energy $(h\nu)$ of doped ZnO thin films in sol gel method.

Table (4.2): The obtained result of the XDR for ZnO nanoparticles at different (pulse, energy, solvent, method).

| Structure	Method to prepare	Solvent type	Energy (mJ)	Pulses	Position (2 theta)	(hkl)	Lattice constant (c) (nm)	FWHM	Crystalline size (nm)	Strain	Dislocation density
Zno/glass	PLA	Methanol	700 mJ	1000	34.85	(002)	5.130902	0.055721	81.83035	0.004234	0.000149
				1500	34.95	(002)	5.12838	0.05721	79.47251	0.00436	0.00015833
				2000	34.45	(002)	5.200524	0.041883	110.1309	0.003146	0.00082443
ZnO/glass		Distilled water	700 mJ	1000	34.74	(002)	5.179515	0.05364	135.9722	0.002548	0.00054087
				1500	34.05	(002)	5.26235	0.05016	193.03823	0.003724	0.0001155
				2000	34.35	(002)	5.217756	0.0643	323.4993	0.001071	0.0009555
ZnO/glass		Methanol	600 mJ	1500	34.90	(002)	5.230902	0.05321	85.56919	0.004049	0.000136573
			700 mJ		34.95	(002)	5.12838	0.05721	79.47251	0.00436	0.00015833
			800 mJ		34.75	(002)	5.12838	0.03721	122.8914	0.00282	0.0006621
ZnO/glass	Sol -gel	-	-	-	34.475	(002)	5.1994	0.0476	96.833333	-0.003578	0.000106647
ZnO/Si					34.425	(002)	5.2067	0.05420	85.16533	0.004069	0.00013781

Chapter Five

Conclusion and Future Works

5.1 Conclusion

Zinc oxide thin film has been successfully prepared on glass and PSi substrates using Pulse laser ablation (PLA) and sol gel methods. The prepared films have hexagonal structure with preferred orientation (0 0 2) and polycrystalline in nature. Additionally, narrow FWHM, low strain and small crystalline size have been obtained. Crystalline size of ZnO dissolved in methanol have been increased with increasing in the Number of laser pulse at fixed of 700 mJ. While, low crystalline size of ZnO dissolved in distilled water at fixed laser pulse of 1500 pulse was obtained at energy of 700 mJ. In addition, the crystalline size of ZnO thin film on glass and PSi substrates were 96.833 nm and 85.165 nm, respectively.

Homogenous film with some cluster and Island, and then the cracking started with increasing of the laser pulses for all cases, expected that the film on glass substrate using PLA method with methanol as a solvent, energy of 700 mJ and pulses of 1500 pulse which revealed Nanostructure like tree leaf. All prepared thin film are free of impurities and contaminations.

All the samples on glass substrates have smooth morphology with transparent in range of 300-800 with high optical band gap energy of 3.37 eV with blue shift toward short wavelength.

5.2 Future works

1- Study the electrical properties of the prepared films.
2- Design of double and multilayer antireflection coating using ZnO.
3- Design single layer antireflection coating using another material such as ZnS and SnO_2.

4- Fabricate ZnO thin film using different physical techniques such DC and RF Sputtering and pulsed laser deposition (PLD).

5- Study the annealing temperature effect on the physical properties of films.

6- Used the films in optoelectronic application such as solar cell, photodetectors and gas sensor.

Reference

Reference

[1] S. Jei Hong and J. In Han"Fabrication of Indium Tin Oxide (ITO) Thin Film withPre-Treated Sol Coating", Journal of Korean Physical Society ,Vol. 45, No. 3, pp. 634-637, September (2004).

[2] P. K. BISWAS, A DE, L K DUA and L CHKODA"Surface characterization of sol–gel derived indium tin oxide films on glass", Indian Academy of Science, Vol. 29, No. 3, pp. 323–330 June (2006).

[3] H. Kim and Y. Kim"Characteristics of Indium-Tin-Oxide Nanoparticles Prepared by Controlled Chemical Coprecipitation Method", Bull. Korean Chem. Soc., Vol. 29, No. 9,(2008).

[4] F. Quarantaa, R. Rellaa and P. Siciliano et al."Preparation and characterization of nanostructured materials for an artificial olfactory sensing system" , Elsevier Science ,Vol. 84,pp. 55–59,(2002).

[5] M. Ivanovkaya "Gas-sensitive properties of thin film heterojunction based on In2O3 nanocomposites" ,Elsevier Science, Vol.7031, PP.1–9,(2003).

[6] J. T. Cox and G. Hass " Triple – layer antireflection coatingon glass for the visible and near- infare" , J.Opt.Soc. Am. 52 (1962) 965.

[7] H.K. Pulker "Characterization of Opticalbthin film", Appl. Opt 18 (1979) 1960.

[8] K.N.Chopra, O.P.Grover, and R. Hradaynath, "Antireflection coating effective at two wavelength simultaneously in the visible region using homogeneously mixed dielectric", Appl. 15 (1979)1750.

[9] R.M.A.Azzam, E. Bu. Habib, J. Casset, G. Chassaing and P. Gravier,"Antireflaction of an absorbing substrate by absorbing thin film at normal incident", Appl. Opt. 26 (1987) 719.

[10] C.L. Negendra, M. Viswanathan, and G. K. M. Thutupalli, "Design and optimization of low – loss wideband antireflection coating for the visible and infrared regions: a new method", Appl. Opt. 14(1985) 1156.

[11] H. A. Macleod, Thin Flim Optical Filters (McGraw-Hill, New York, 1986).

[12] K. L. Chopra,Thin – Flim Phenmena (McGraw – Hill, New Yrk, 1989).

[13] J and W, Fundmentals of Optics (McGraw – Hill Koganasha, Ltd, 1984)

[14] A. Hashim, M. S. Jaafar, A. J. Ghazai, N. Alrawi," Fabrication and characterization of ZnO thin film using sol–gel method". International Journal for Light and Electron Optics 124(6):491–492 · March 2013.

[15] A. Mussetand A, Thelen, "Multilayer antireflections, in progress in optics" E. Wolf, ed (North – Holland, Amsterdam,1970), Vol. 18, p p. 201-233.

[16] A. Thelen, Design of Optical Interference Coating McGraw – Hill Compqny, New York, 1989)

[17] H. Gh. Rashid, Z. T. Al- Dahan, and H. M. Ibrahim, "Design of dual – band antireflection coating", accepted in the first conference on Physics and materials research IAEC, Baghdad, 1999.

[18] K. Robinvitch and A. Pagis "Influence of heat treatments on the spectral performance of a V –type double antireflection coating at 1.06 μm", Appl. Opt. 21(1982) 2160.

[19] H. L. Hartnagel, A.L.D., A. K. Jain, and C. Jagadish, Semiconducting Transparent Thin Films. 1995, Bristol: Institute of Physics. 358.

[20] U.A. Ozgur, , Y. I. Liu, C. Teke, A. Reshchikov, M. A. Dogan, S. Avrutin, V. Cho, S. J. and Morkoc, H., A comprehensive review of ZnO materials and devices. Journal of Applied Physics, 2005. 98(4): p. 103

[21] L. Kazmarski and A. H .Clark, "Polycrystalline and Amorphous Thin Films and Device", Edited by Lawrence Academic Press, New York, (1980).

[22] A.V. SIngh, M. kumar, R. M. Mehra, A. Wakahara and A.Yoshida," Al-doped zinc oxide (ZnO:Al) thin films by pulsed laser ablation". J. Indian Inst. Sci., Sept –Oct. 2001, 81, 527-533.

[23] Y. Ishikawa, Y. Shimizu, T. Sasaki and N. Koshizaki," Preparation of zinc oxide nanorods using pulsed laser ablation in water media at high temperature". Journal of Colloid and Interface Science 300 (2006) 612–615

[24] Q.H. Chen and W. G. Zhang," Successive preparation of decorated zinc oxide organic sol by pulsed laser ablation and their luminescence characteristics". j.apsusc.2006.06.065.

[25] R.K. Thareja and S. Shukla, "Synthesis and characterization of zinc oxide nanoparticles by laser ablation of zinc in liquid. Applied Surface Science 253 (2007) 8889–8895.

[26] R. S. Ajimsha, G. Anoop, A. Aravind, and M. K. Jayarajz," Luminescence from Surfactant-Free ZnO Quantum Dots Prepared by Laser Ablation in Liquid". Electrochemical and Solid-State Letters, (2008), 11 (2) K14-K17.

[27] J. M. Cho, J. K. Song, and S. M. Park," Characterization of ZnO Nanoparticles Grown by Laser Ablation of a Zn Target in Neat Water". Bull. Korean Chem. Soc. 2009, Vol. 30, No. 7.

[28] I.S. Virt, I.V. Hadzamana, I.S. Bilyka, I.O. Rudyic, I.V. Kuriloc And et al. "Properties of ZnO and ZnMnO Thin Films Obtained by Pulsed Laser Ablation", Oxide Materials for Electronic Engineering" (OMEE-2009), Vol. 117, No. 1. 2010.

[29] R. A. Ismail, A. K. Ali, M. M. Ismail, K. I. Hassoon." Preparation and characterization of colloidal ZnO nanoparticlesusing nanosecond laser ablation in water". 1:45–49. Appl Nanosci (2011).

[30] G Atanasova1, A Og Dikovska, M Stankova, P Stefanov1 and P A Atanasov. " XPS study of ZnO nanostructures prepared by laser ablation". Journal ofPhysics:ConferenceSeries 356 012036. (2012).

[31] D. Nakamura, T. SImogaki, K. Okazaki, M. Higashihata, H. Ikenoue and et al," Synthesis of Various Sized ZnO Microspheres by Laser Ablation and Their Lasing Characteristics". JLMN-Journal of Laser Micro/Nanoengineering,Vol. 8, No. 3, (2013), .

[32] F. A. Fadhil and I. H. Hadi, " Preparation and characterization of zinc oxide nanoparticles by laser ablation of zinc in isopropanol". Eng. &Tech, Vol.33 , Part (B), No.5, Journal, (2015).

[33] E. T. Salim, M. A. Fakhri, ,H. Hassan, Z. T. Salim and A. Z. Mohamed, "PhysicochemAical properties of ZnO Nanoparticles prepared using low energy low repetition rate Laser system" . Sci.Int. (Lahore), 28(5), 4501-4506(2016).

[34] S. V. Farahan, A. Mahmood and M. Goranneviss, " The effect of laser environment on the characteristics of ZnO nanoparticles by laser ablation". Int Nano Lett 6:45–49, (2016).

[35] R. A. Ismail, N. F. Habubi, E. H. Hadi, "Synthesized and characterization of pure and Er+3 doped ZnO nanoparticles by using laser ablation in ethanol". World Scientific News 33 67-78(2016), .

[36] K. S. Khashan and F. Mahdi, " Synthesis of ZnO: Mg Nanocomposite by Pulsed Laser Ablation in liquid". Surf. Rev. Lett. 0, (2017), 1750101.

[37] A.R. Phani, M. Passacantando, and S. Santucci, "Synthesis and characterization of zinc aluminum oxide thin films by sol-gel technique". Materials Chemistry and Physics, 68, pp. 66-71, (2001).

[38] K.R. Murali, Properties of sol-gel dip-coated zinc oxide thin films. *Journal of Physics and Chemistry of Solids, 68*, pp. 2293-2296,(2007).

[39] Z. Xiaofeng, J. Tao, Z. Jian and W. Xiaohua, "Humidity sensor based on quartz tuning fork coated with sol-gel-derived nanocrystalline zinc oxide thin film". Sensors and Actuators B,123, pp.299-305,(2007).

[40] P. Bhattacharyya, P. K. Basu, H. Saha, and S. Basu, "Fast response methane sensor using nanocrystalline zinc oxide thin films derived by sol-gel method". Sensors and Actuators B,124, pp. 62-67,(2007). .

[41] C. Mehmet, O. Shine, and C. Gabriel, "Sol-gel synthesis, comparative characterization, and reliability analyses of undoped and Al-doped zinc oxide thin film". Thin Solid Films, 517, pp. 6323-6326,(2009). .

[42] C. Jagadish, and S. J. Pearton, "Zinc Oxide Bulk, Thin Films, and Nanostructures: Processing, Properties, and Applications". Elsevier, Netherlands. (2006).

[43] O. Shane, C. Mehmet, Paul, T. G. Mark, A. Jeff, P. Ian et al. "The effect of dopants on the morphology, microstructure and electrical properties of transparent zinc oxide films prepared by the sol-gel method". Thin Solid Films, 520, pp. 1174-1177, (2011). .

[44] M. Sathya, A. Claude, P. Govindasamy and K. Sudha. "Growth of pure and doped ZnO thin films for solar cell applications", Advances in Applied Science Research, 3 (5):2591-2598, 2012 .

[45] L. Yang, B. Duponchel, R. Cousin, C. Gennequin, G. Leroy, J. Gest, et al. "Structure, morphology and electrical characterizations of direct current sputtered ZnO thin films". Thin Solid Films, 520, pp. 4712-4716(2012).

[46] Y. Al-Douri, A. H. Reshak, W. K. Ahmed, A. J. Ghazai "Structural and optical investigations of In doped ZnO binary compound" Materials Express 4, 159-164, (2014) .

[47] A. J. Ghazaia, E. A. Salmanb, Z. A. Jabbarc." Effect of Aluminum Doping on Zinc Oxide Thin Film Properties Synthesis by Spin Coating Method". American Scientific Research Journal for Engineering, Technology, and Sciences (ASRJETS) Volume 26, No 3, pp 202-211, (2016).

[48] A. J. Ghazai1, E. A, Salman and Z. H. ------." Structural Properties of Zno Thin Films Prepared Using Different Techniques". Swift Journal of Physical Sciences Vol 2(1) pp. 001-004 May, 2016.

[49] M. Born and E. Wolf, Principle of Optics, 5th – ed. Program on London, 1975.

[50] Z. Knittle, Optics of Thin – Flim (Wily, New York, 1976).

[52] M. Aziz, S. S. Abbas and W. Rosemaria "Size-controlled synthesis of SnO2 nanoparticles by sol–gel method", Materials Letters, Vol. 91, PP. 31–34, (2013).

[53] N. Nadaud," Structural studies of tin-doped indium oxide (ITO) and In4Sn3O12", J. Solid State Chem, Vol. 135, No. 1, pp. 140-148, (1998).

[54] R.Savu, M. Adlfo and E. Joanni," grain size effect on the electrical response of SnO2 thin and thick film gas sonsor", Materials research, Vol.12, NO.1, P.83-87, (2009).

[55] R. Chandran and G. Suresh, "A comparative study of physical and optical properties pf cdZnS and cdNiS Nanocrystalline films deposition by chemical bath method", Chalcogenide Lett ., Vol.8, No.11 ,pp. 689-694,(2011).

[56] F. O. Adurodija, L. Semple and R. Bruning, "Crystalliza- tion Process and Electro-Optical Properties of In2O3 and ITO Thin Films", Journal of Materials Science, Vol. 41, No. 21, pp. 7096-7102,(2006).

[57] S. A. Bashar, "Study of Indium Tin Oxide (ITO) for Novel Optoelectronic Devices", University of London Regulations for the Degrees of M.Phil. and Ph.D., October (1997).

[58] Y. V. Gassenbauer and A. Klein, "Electronic and Chemical Properties of Tin-Doped Indium Oxide (ITO) Surfaces and ITO/ZnPc Interfaces Studied In-situ by Photoelectron Spectroscopy", J. Phys. Chem,Vol.110, pp.4793-4801,(2006).

[59] XRD picture. Available from:

 http://tap.iop.org/atoms/xray/530/img_full_47305.gif.

[60] T. Ungar, Microstructural parameters from X-ray diffraction peak broadening. Scripta Materialia 51, 777–781, (2004).

[61] G. Maeder, X-ray diffraction and stress measurements. Chemica Scripta a 26, 23–31, (1986).

[62] P. Pourgahramani, and P. Bal´aˇz, "Structural Changes and Characterizations in the Powder Materials Obtained From Milling Processes. In: M. Yekeler (Ed.) Powder Technology and Characterization. Trivandrum, Kerala, pp. 217–250, (2008)

[63] T. Berg, E. Marosits, J. Maul1, P. Nagel, U. Ott, F. Schertz, S. Schuppler, Ch. Sudek and G. Schönhense, "Quantum Confinement Observed in the X-ray Absorption Spectrum of Size Distributed Nanodiamonds Extracted From the Murchison Meteorite", Lunar and Planetary Science XXXIX (2008).

[64] T. Ogawa and Y. Kanemitsu "Optical Properties of Low-Dimensional

Materials", Word Scientific, Singapore, (1995).

[65] S. Boninelli, "Properties and Evolution of Si Nanoclusters Studied by Energy Filtered Transmission Electron Microscopy", University of Catania, Ph.D thesis, December (2004).

[66] P. Harrison, "Quantum Wells, Wires and Dots", John Wiley & Sons, LTD., (2004).

[67] Y. Dan, S. Evoy and A. Johnson,"Chemical Gas sensors Based on nanowires", Arxiv preprint arXiv:0804. 4828 (2008).

[78] J. Schaffer, A. Saxena, S. D. Antolovich, T. H. Sanders Jr. and S. B. Warner: The Science and Design of Engineering Materials, 2nd ed.,

(McGraw-Hill International, pp. 65–75, (1999).

[69] A. Alivisatos,"Semiconductor Clusters, Nanocrystals, and Quantum Dots. Science", 271, 933-937, (1996).

[70] A. Ivashchenko , and I. Kerner , "Moldavian J. Phys. Sci. ", "Physical Approaches to Improvement of Semiconductor Gas Sensor Based on SnO2 Thin Films" Moldavian Journal of the Physical Sciences, Vol. 2, N1, , PP.95-102, (2003).

[71] V. Satish, Kailas, "Material Science", Dept. of Mechanical Engineering, Indian Institute of Science, Bangalore, India, (2005).

[72] J. Van Berkum , A. C. Varmcuch , R. Delhen , Th. H. Dinkeijser , and E. J. Hemeijer , "Applicabilities of the Warren-Averbach analysis and an Alternative Analysis for Separation of Size and Strain Broadening," J. Appl. Crys., Vol. 27, , PP. 345-357, (1994).

[73] T. Obata , K. Komeda , T. Nakao , H. Ueba , and C. Tasygama , "Structural Characterization of Si0.7Ge0.3 Layers Grown on Si(001) Substrates by Molecular Beam Epitaxy," J. Appl. Phys. Vol. 81, P.199, (1997) .

[74] S. Hussain, "Investigation of Structural and Optical Properties of Nanocrystalline ZnO", Thesis Report, Linköpings Universitet, (2008).

[75] S. T. Ngqondo , "Hydrothermally grown Pb2+ doped ZnO Nanorods for Hydrogen and Acetylene Gas sensing" Department of Physics, University of Zululand, 2008.

[76] C. R. Blanchard "Atomic Force Microscopy", the Chemical Educator, Vol. 1, No. 5, P 5059, 1996.

[77] F. Guo, B. Yang, Y. Yuan, Z. Xiao, Q. Dong, Y. Bi and J. Huang," A Nanocomposite Ultraviolet, 2001.

[78] J. Goldstein (2003). Scanning Electron Microscopy and X-Ray Microanalysis. Springer. ISBN 978-0-306-47292-3. Retrieved 26 May 2012.

[79]Jump up ^ Joseph Goldstein (2003). Scanning Electron Microscopy and X-Ray Microanalysis. Springer. ISBN 978-0-306-47292-3. Retrieved 26 May 2012.

[80] R. J. Elliot and A. I. Gibson, "An Introduction to Solid State Physics and Application", 1st edition, Macillian Inc. (1974).

[81] R. A. Grenier, "Semiconductors Device, Electronic Energy Series", Mc Graw-Hill, Book Co.Inc. (1961).

[82] L. Kazmarski and A.H.Clark, "Polycrystalline and Amorphouse Thin Films and Device", Edited by Lawrence Academic Press, New York, (1980).

[83] G. Burns, "Solid State Physics, Academic Press, Inc.", Harcourt Brace Jovanovich, New York, (1985).

[84] M. Grundmann, H.v. Wenckstern, R. Pickenhain, Th. Nobis, A. Rahm, M. Lorenz, "Super lattices and Microstructures", Vol. 38, , PP. 317–328, (2005).

[85] M. Lorenz, H. Hochmuth, R. Schmidt, E. M. Grund, M. Kaidashev, Grundmann, "Advances of Pulsed Laser Deposition of ZnO Thin Films", Ann. Phys., V. 13, , P. 59, (2004).

[86] J. Taus, "Amorphous and Liquid Semiconductors", Plenums Press, New York and London, (1974).

[87] T. S. Moss, "Optical Properties of Semiconductors", London Butter Worthes Scientific Puplications, (1959).

الملخص

في هذا البحث تم تصميم وتحضير طبقة مفردة من طلاء مضاد لانعكاس من اغشية أوكسيد الزنك النقية على ارضيات أساس من الزجاج والسيليكون المسامي باستخدام طريقتي القشط بنبضات الليزر والطلاء البرمي.

يقسم العمل الى جزئيين أساسيين هما الأول.. تصميم طلاء مضاد للانعكاس في طبقة مفردة من اغشية أوكسيد الزنك الرقيقة باستخدام المصفوفة المميزة المعدلة لتحقيق شرط الانعكاس الصفري نظريا.

والثاني.. تحضير اغشية أوكسيد الزنك النانوية على ارضيات أساس مختلفة بطريقتي PLA والتي تضمنت دراسة تأثير عدد الضربات 1000,1500,2000 ضربة، الطاقة المستخدمة 600,700,800 mJ ونوع المذيب (ماء منزوع الايون) والميثانول، وكذلك نوع الأرضية الأساسي وبالإضافة إلى ذلك، تم استخدام طريقة الطلاء البرمي (spin coating) لترسيب هذا الغشاء.

تم دراسة الخصائص التركيبية والبصرية للأغشية المحضرة باستخدام جهاز حيود الاشعة السينية (XRD)، المجهر الالكتروني الماسح (SEM)، و مطياف تشتت اشعه سينية (EDX)، ومطياف UV–Vis على التوالي.

نتائج XRD أظهرت ان اغشية أوكسيد الزنك المحضرة هي بتركيب سداسي متعدد التبلور مع اتجاه سائد (002) بالإضافة لذلك فان حجم البلوري ازداد مع زيادة عدد نبضات الليزر مع الميثانول و الماء الايوني كمذيب وعند طاقه ثابته 700 mJ. باستثناء عند عدد نبضات ١٥٠٠ نبضه و طاقه 700 mJ مع الميثانول كمذيب فان الحجم البلوري هنا اصبح اقل ما يمكن وظهور حاله نانو. اضافه لذلك فان الأغشية المترسبة على ارضيات الأساس من الزجاج والسيلكون المسامي باستخدام طريقه الطلاء البرمي تمتلك حجما بلوريا and 85.165 nm (96.833) على التوالي. عرض النطاق عند منتصف أعظم شده FWHM ضيق ولم يتم ملاحظه أي تغيير في الطور لجميع الحالات.

صور المجهر الالكتروني الماسح SEM أوضحت ان الأغشية في كل الحالات كانت متجانسه مع بعض الجزر والتكتلات بعدها يبدا ظهور التشققات وتزداد بزياده عدد النبضات باستثناء الغشاء المرسب على الزجاج باستخدام طريقه PLA مع محلول الميثانول بطاقه mJ 700 وعدد نبضه ١٥٠٠ نبضه والتي أوضحت تركيبا نانويا يشبه ورق الشجر.

اما نتائج EDX فقد بينت ان الاغشية المحضرة خالية من الشوائب وهذه النتائج تتطابق مع النتائج XRD.

وكانت نتائج UV-Vis الخصائص البصرية متضمنة السلوكية البصرية، فجوة الطاقة البصرية ومعامل امتصاص كدالة للطول الموجي أوضحت ان الاغشية المحضرة تمتلك نفاذية عالية بحدود 85% في المنطقة المرئية والتي مداها يتراوح بحدود 300-800 nm مع فجوة طاقة بصرية كبيرة نسبيا بحدود 3.37 eV مع حصول انحراف باتجاه الاطوال الموجية ... عند زيادة الضربات والطاقة.

جمهورية العراق
وزارة التعليم العالي والبحث العلمي
جامعة النهرين
كلية العلوم
قسم الفيزياء

تصميم وتصنيع غشاء رقيق من اكاسيد الزنك المضاد للانعكاس باستخدام تقنيات مختلفة

رسالة
مقدمة الى كلية العلوم \ جامعة النهرين
كجزء من متطلبات نيل درجة ماجستير في علوم الفيزياء

من قبل

نداء طه ياسين
بكالوريوس الجامعة المستنصرية ٢٠٠٥

بأشراف

أ.م.د. علاء جبار غزاي

شوال ١٤٣٨   تموز ٢٠١٧